2007-01-01

Modeling and Evaluation of Personal Displacement Ventilation System for Improving Indoor Air Quality

Yue Xu
University of Miami, y.xu6@mycanes.miami.edu

UNIVERSITY OF MIAMI

MODELING AND EVALUATION OF PERSONAL DISPLACEMENT VENTILATION SYSTEM FOR IMPROVING INDOOR AIR QUALITY

By

Yue Xu

A THESIS

Submitted to the Faculty
of the University of Miami
in partial fulfillment of the requirements for
the degree of Master of Science

Coral Gables, Florida

December 2007

UNIVERSITY OF MIAMI

A thesis submitted in partial fulfillment of
the requirements for the degree of
Master of Science

MODELING AND EVALUATION OF PERSONAL DISPLACEMENT VENTILATION SYSTEM FOR IMPROVING INDOOR AIR QUALITY

Yue Xu

Approved:

Dr. Xudong Yang Associate Professor of Civil, Architectural, and Environmental Engineering	Dr. Terri A. Scandura Dean of the Graduate School
Dr. Helena Solo-Gabriele Professor of Civil, Architectural, and Environmental Engineering	Dr. Gecheng Zha Associate Professor of Mechanical and Aerospace Engineering

Yue Xu (M.S., Architectural Engineering)
Modeling and Evaluation of Personal Displacement Ventilation System for Improving Indoor Air Quality (December 2007)

Abstract of a thesis at the University of Miami.

Thesis supervised by Professor Xudong Yang.
No. of pages in text. (85)

This research aims at evaluating a new ventilation concept: personal displacement ventilation (PDV) for improving indoor air quality. The new ventilation method combines room displacement ventilation with task ventilation, the latter being directed at controlling air quality and comfort in the microenvironment where the building occupant is working, with the premise that such directed ventilation will maintain air quality where it matters. This approach could lead to improved ventilation system design that could even provide individual control of indoor microclimate.

The effectiveness of PDV was studied by using computational fluid dynamics (CFD) modeling and rigorous validation experiments. First, a small office setup was built in a controlled environmental chamber. Three PDV cases with different locations of contaminant source and one general displacement ventilation (DV) case were investigated. Spatial distributions of airflow, temperature, and hypothetical pollutant distributions were measured. The measured data were then used to evaluate the performance of PDV against defined indoor air quality and thermal comfort criteria, and to validate the CFD model. The validated CFD program was further used to study PDV under various conditions.

This study found that basic equipped PDV acts no different from DV from airflow pattern's point of view. Due to the lack of heat generation around occupant's legs, local buoyancy effect is not strong enough to attract supply air, which is generated from diffuser nearby, to join in the plume around occupant. However, auxiliary activities adjusting the direction of supply air and adding high panels around person can improve the fraction of supply air to join the plume around person or decrease the average contaminant concentration in breathing zone.

ACKNOWLEDGEMENT

I would like to gratefully acknowledge my advisor, Professor Xudong (Don) Yang, for his tireless guidance and support in both of my study and life. He has always given me valuable suggestions and encouragement throughout the completion of my Master's study. His knowledge and high level in research have helped me build up my research experience from where I will benefit in my whole life.

I would also like to thank my thesis committee members, Professor Helena Solo-Gabriele and Professor Gecheng Zha. Their critical comments and suggestions have been very helpful to the completion of this work.

My thanks extend to Professor Jelena Srebric and Brendon J. Burley in Penn State University for their generous support in the experiments.

Finally, I am forever indebted to my parents for their understanding, trust, precious advice and encouragement. And I am also grateful to my labmate (Wei Yan) for his help.

TABLE OF CONTENTS

LIST OF FIGURES

LIST OF TABLES

Chapter 1 Introduction

1.1 Problem statement

Buildings have been provided as shelters from out door climate like wind, rain, sunshine and cold ever since human civilization was established thousands of years ago. As industry developed in the mid 19th century, people spent more and more time in indoor environments i.e., offices, schools, public buildings, homes etc. Thus, to date, buildings are required for more needs; for instance, indoor air quality, thermal comfort, and other parameters reflect the assessment of indoor environment occupied by people.

Since many people spend more than 90% of their time in an artificial climate (Turiel, 1985, Awbi, 1991), indoor environment is very important to health and welfare. It's been reported that between 800 and 1,200 thousand buildings in the United States are the worksites to millions of workers where indoor environmental problems have arisen. Although the specific agents associated with these problems are not known, many studies have demonstrated that these symptoms, illnesses and complaints are related to poor indoor air quality and perceived physical discomfort.

Ventilation has the most significant effect and consequences on the quality of indoor air. The two well-known conventional ventilation systems are mixing and displacement ventilation. They are easy designed and widely used in practice. However, neither of them can provide the required specifications for individual control and the condition of a small volume around the occupant which is called micro-environment. To solve this problem, another ventilation supply method- task ventilation system which can provide occupants with improved thermal comfort, air quality and individual control of

micro-environment was proposed (Fanger, 1999). Whereas, this improved method also has its defect which is that the direct supply of fresh air to breathing zone can disturb the buoyancy-driven natural convection plume and lead to thermal discomfort (Gao, 2004). There is a need for improved systems that can eliminate or mitigate building-related health problems and supply more comfortable and healthy micro-environment.

1.2 Status of research

This section includes a discussion of conventional and recently explored ventilation strategies including mixing ventilation, general displacement ventilation (DV), task ventilation and personal displacement ventilation (PDV).

Ventilation methods

Heating, ventilating, and air-conditioning (HVAC) systems are used to create an indoor environment with acceptable air temperature, humidity, air movement and to maintain freshness of indoor air. Unfortunately, ineffective ventilation of the indoor air space has been blamed as a major factor impacting indoor air quality. Since 1971, the Hazard Evaluations and Technical Assistance Branch of the NIOSH has conducted over 500 indoor air quality investigations in response to complaints associated with poor indoor air quality. In over half (52%) of these investigations, deficient building ventilation systems or improper operation of these systems was believed to be the most likely cause of building occupant complaints (Salisbury 1989; Seitz 1989).

The most commonly used types of ventilation systems in the U.S. are mixing ventilation, where the system tries to mix up all the air in a room, producing a uniform

temperature throughout the space and diluting the pollutants (Figure 1.1a). The conditioned air in a mixing system is normally discharged from air outlets at velocities much larger than those acceptable in the occupied zone. The diffuser jets mix with the ambient room air by entrainment and create relatively uniform air flow, temperature, and air quality conditions in the occupied zone. While mixing does dilute pollutants, it also sweeps them away from their sources and distributes them throughout the room. Moreover, this approach can also result in dead spaces depending on the location of intakes and registers and room geometry, as well as non-uniform distributions of air, unless large airflows are used with a consequent effect on energy expenditures and thermal comfort.

In order to improve the indoor air quality, DV has received considerable attention recently. Contrary to the traditional mixing ventilation, DV seeks to prevent mixing rather than cause it. In the side-wall-supply DV system (Figure 1.1b), conditioned air with a temperature slightly lower than the desired room air temperature is supplied from air outlets at low air velocities (less than 0.5 m/s). The outlets are located at or near the floor level, and the supply air is directly introduced to the occupied zone. Return grilles are located at or close to the ceiling through which the warm room air is exhausted from the room. The supply air spreads over the floor and then rises as it is heated by the heat sources in the occupied zone. Heat sources (e.g., occupants, computers) in the occupied zone create upward convective flows in the form of thermal plumes. These plumes remove heat and contaminants from the surrounding occupied zone. Two distinct zones are thus formed within the room, one lower zone below the stratification level with displacement flow, and one upper zone with mixing.

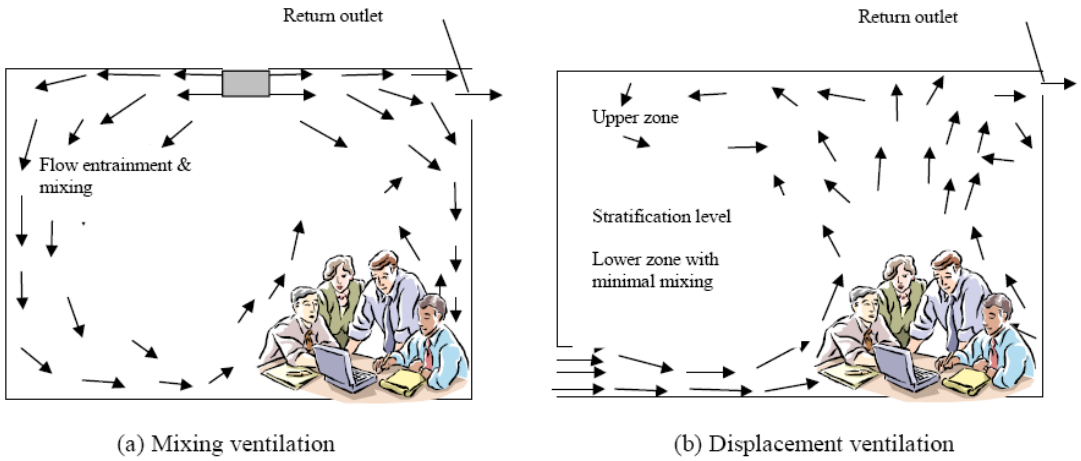

Figure 1.1 Typical room ventilation systems

The objective of DV is to create conditions in the occupied zone close to the supply air conditions. However, care must be taken when the pollutants are generated from a large area source on the lower level such as from the floor, where the supply air may become contaminated before reaching the occupied zone (Yang and Srebric 2001).

Ventilation techniques for the entire room volume as mixing or DV cannot provide the required specifications for individual control and the condition of a small volume around the occupant (the microclimate). Furthermore, centrally controlled air conditioning systems ignore the apparent differences in thermal comfort requirements between persons (Benzinger 1979). As alternatives, task ventilation systems intend to influence only the immediate surroundings of the person operating the system (Krantz 1984; Bauman et al. 1994; Bauman and Arens 1996). These systems create a microclimate within a macroclimate by introducing the (fresh) supply air near the workplace close to the occupant. As a result of having local zones, strict health and comfort related requirements for the air conditioning of the macroclimate may be mitigated. However, these systems normally introduce the air from relatively small

diffusers at relatively high velocity and turbulence intensity. Thus, they possess a potential risk of draft to the occupants (Figure 1.2a).

PDV concept intends to combine the positive features of DV with those of task conditioning. The major objective of this principal is to create a healthy and comfortable micro-environment within a macro-environment. Because the air is supplied directly to the occupied zone, the air quality near the occupant could be improved. Meanwhile, PDV applies the rules set by the DV principle, i.e., introduction of sub-cooled air (supply temperature only slightly lower than room temperature) over a relatively large area at low velocity (e.g., 0.2 m/s), the specific comfort requirement of the occupant may be individually controlled and satisfied. Figure 1.2b shows one type of PDV system (desk displacement ventilation). Loomans (1998) investigated such a system with regard to micro/macroclimate and thermal comfort and concluded that comfort conditions can be achieved with desk displacement ventilation. Unfortunately, his study did not include air pollutant and is thus limited.

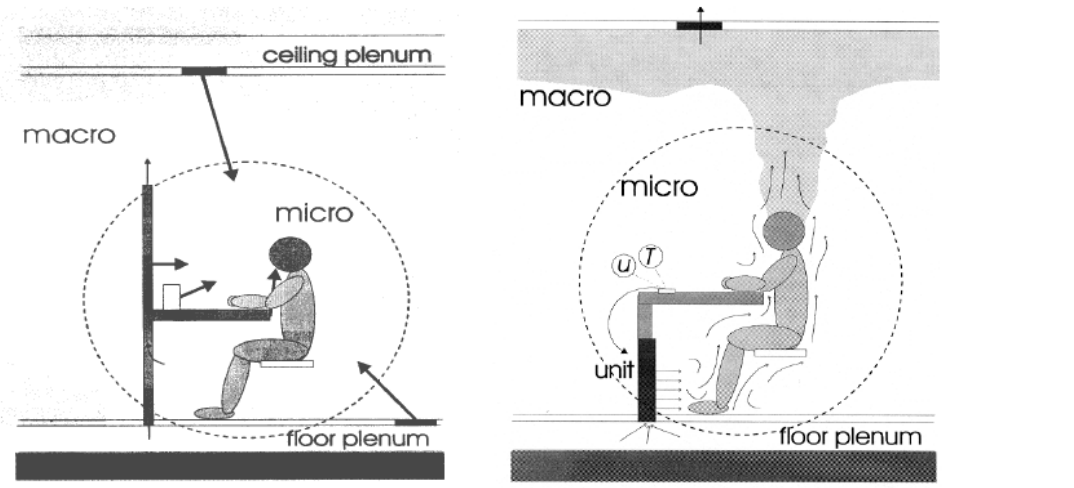

(a) Task conditioning system (b) Personal (desk) displacement ventilation system

Figure 1.2 Illustration of task conditioning and PDV systems (Loomans 1998)

1.3 Objectives and approaches

As discussed in the previous section, conventional ventilation systems cannot meet all the requirements for thermal comfort, air quality and individual control of micro-environment. A well-performed ventilation system is in great need to solve all these problems raised as occupants call on more healthy and comfortable micro-environment.

The objectives of this thesis are to evaluate the new ventilation concept: PDV for improving indoor air quality by using computational fluid dynamics (CFD) modeling and rigorous validation experiments. A small office setup using PDV is built in a controlled environmental chamber and spatial distributions of airflow, temperature, and hypothetical pollutant distributions are measured. The measured data are used to validate the CFD model. The validated CFD program will then be used to further study and quantify the design of PDV under selected source configurations, ventilation designs, and load conditions. Based on the experimental and simulation results, reasonable recommendations for the use of PDV are discussed.

1.4 Outline of thesis

This thesis contains six chapters.

Chapter 1 briefly discusses the problems that current ventilation systems have performed and sets the objectives of this research.

Chapter 2 provides an overview of current study on PDV and DV systems.

Chapter 3 reports experimental study on the performance of PDV and DV systems with regard to airflow pattern, temperature distribution and contaminant concentration.

Chapter 4 focuses on validation of CFD model. Comparison between simulation and experimental results is discussed in this chapter.

Chapter 5 presents 6 PDV cases in addition to the four experimental cases. Validated CFD model is applied to simulate these cases. Evaluation of these cases is achieved with two indicators: ventilation bypass factor and local average concentration.

Finally, Chapter 6 summarizes the major conclusions out of this research and provides recommendations for future work in this area.

Chapter 2 Literature Review

2.1 Introduction

As more and more attention has been given to air quality, thermal comfort and self-control of micro-environment around occupants in public buildings, general criteria, such as supply and exhaust conditions, number of air changes and ventilation effectiveness, are not sufficient to evaluate micro-environmental conditions. To analyze and predict detailed micro-climate conditions, two main approaches are commonly used: experimental measurement and computer simulation.

Many experimental and simulation work have been done to investigate airflow pattern, temperature and concentration distribution in DV systems. For example, Yuan et al. (1999) provided experimental data of DV for a small office, a large office with partitions, and a classroom with regard to airflow pattern, temperature and concentration distribution. Dickson D. (1994) reported experimental results regarding displacement and mixing ventilation from EA Technology. It was shown that the room air temperature distribution was uniform for both systems, although temperature profiles were strongly dependant on the supply air temperature when using DV. Loomans (1998) investigated PDV system with regard to micro/macroclimate and thermal comfort and concluded that comfort conditions can be achieved with PDV. Unfortunately, his study did not include contaminant concentration and is thus limited.

Local contaminant concentration is an important indicator to evaluate indoor air quality. However, local concentration in occupied zone is very sensitive and difficult to predict. For instance, types and locations of contaminant source can greatly affect local

concentration. Contaminant distributions from fixed local point sources (Yuan et al. 1999; Srebric and Chen 2002; Brohus and Nielsen 1996; Hagstrom et al. 2002) or a small area source (Hagstrom et al. 1999; Cheong et al. 2003) have been widely studied using both experimental measurements and computational fluid dynamics (CFD) modeling. Brohus and Nielsen (1996) studied the effect of source height on personal exposure and found that when the source is passive (not associated with heat sources), the perceived personal exposure varies significantly with the elevation of the source. And when it is located at lower level, the occupant plume may bring the contaminants from the lower level to the breathing zone and thus make the air quality worse at the breathing zone. In another study, Hagstrom et al. (1999) investigated the effect of uniformity of heat sources and contaminants on contaminant distributions. They found that the nonuniform distribution of heat and contaminant sources has a remarkable influence on the contaminant removal efficiency and that the influence depends on the air supply method. Recently, He et al. (2005) And Yang et al. (2004) found that both ventilation method and source types and locations can significantly affect local contaminant distributions. Even when the contaminant source is at floor level (i.e., unfavorable source location), DV can still generate slightly lower concentration at or below the breathing zone compared to completely mixing ventilation. In some cases, the higher efficiency of contaminant removal could be reached with proper placement of supply and exhaust diffusers. The general exposure level could be estimated through analyzing the relative source positions in the airflow path. The location of the exhaust diffuser may not greatly affect the airflow pattern, but it can significantly affect the exposure level in the room.

Lau and Chen (2007) studied a workshop with floor-supply DV. It was found that indoor air quality can be improved because the contaminant concentration in the breathing zone is lower than that of mixing system. Since a more unidirectional flow was created, the slow recirculation at the occupied zone was eliminated for the floor-supply ventilation, and the risk of cross-contamination can be effectively reduced.

DV combined with other systems for practical use has also been investigated. Bunn et al. (1991) reported a CFD and laboratory investigation on a combined system of displacement and chilled beams. It was found that the buoyancy produced by the displacement principle was enhanced by chilled beams.

Comparing to the plenty of research have been done on DV, PDV study on indoor air quality in literature is very few and incomplete. In our study, we will present a set of experiments on PDV regarding airflow, temperature and concentration distribution. The experimental data will be used to validate CFD model which has been applied for further study.

2.2 CFD models

CFD approach can provide detailed information of airflow, temperature and contaminant distributions by solving a series of conservation equations, for example, momentum, heat transfer and pollutant transport. With regard to solution of these governing equations, turbulence model, discretisation technique, grid generation methods and boundary condition should be introduced.

2.2.1 Governing equations

Fluid flow field can be described by a combination of continuity equation, momentum equations and other related equations such as energy and pollutant transport equation. In this study, air flow is assumed to be ideal, incompressible and steady state.

Continuity equation

$$\frac{\partial}{\partial x_i}(\rho u_i) = 0 \tag{2.1}$$

where

ρ = Density of the fluid, (kg/m3)

u_i = Velocity component (u, v, w), (m/s)

x_i = Coordinate axis (x, y, z) (m)

Momentum equations

Momentum equations are derived from Newton's second law on a finite fluid volume acted by surface forces and volume forces.

$$\frac{\partial}{\partial x_j}(\rho u_i u_j) = \frac{\partial}{\partial x_j}\left[\mu(\frac{\partial u_i}{\partial x_j} + \frac{\partial u_j}{\partial x_i}) - \rho\overline{u_i' u_j'}\right] - \frac{\partial p}{\partial x_i} + B_i + S_u \tag{2.2}$$

where

p = Pressure (N/m^2 or Pa)

μ = Kinetic viscosity (kg/ms)

u_i' = Fluctuating velocity component (u' , v' , w')

B_i = Volume force component (N/m^3)

S_u = Source term (N/m^3)

The left side of equation (2.2) is convection term. And the right side is consist with diffusion term indicating the influence of shear forces, pressure gradient term, buoyancy term (volume force) and source term.

$-\rho\overline{u_i'u_j'}$, called Reynolds stresses, are introduced when converting the instantaneous variables into mean conservation equations. It could be determined by assuming the turbulent stresses are proportional to the mean velocity gradients.

$$-\rho\overline{u_i'u_j'} = \mu_t\left(\frac{\partial u_i}{\partial x_j}+\frac{\partial u_j}{\partial x_i}\right)-\frac{2}{3}\rho k\delta_{ij} \tag{2.3}$$

where

μ_t = Turbulent or eddy viscosity (kg/ms)

k = Turbulent kinetic energy (J/kg)

δ_{ij} = Kronecker delta

Buoyancy term (B_i) could be determined by Boussinesq approximation (Arpaci and Larsen, 1984)

$$B_i = -\rho\beta g_i(T-T_{ref}) \tag{2.4}$$

where

β = Cubic expansion coefficient (1/K)

g_i = Gravitational acceleration component (m/s^2)

T = Fluid temperature (℃)

T_{ref} = Reference temperature (℃)

Energy equation

Energy equation describes the temperature distribution in entire fluid domain. It is developed from the first law of thermodynamics.

$$\frac{\partial}{\partial x_i}(\rho u_i c_p T) = \frac{\partial}{\partial x_i}(\lambda \frac{\partial T}{\partial x_i}) + S_T \tag{2.5}$$

where

c_p = Specific heat of fluid (J/kg℃)

T = Mean temperature of fluid (℃)

λ = Thermal conductivity, the sum of laminar and turbulent conductivity (W/m^3)

S_T = Source term (W/m^3)

Concentration equation

$$\frac{\partial}{\partial x_i}(u_i c) = \frac{\partial}{\partial x_i}(D \frac{\partial c}{\partial x_i}) + S_c \tag{2.6}$$

where

c = Concentration of contaminant (kg of contaminant / kg of air)

D = Thermal diffusivity, the sum of mass molecular diffusivity and turbulent diffusivity (m^2/s)

S_c = Source term (kg of contaminant / kg of air·s)

2.2.2 Turbulence model

There are a lot of turbulence models to determine the turbulent viscosity μ_t. One of the earliest and most popular turbulence models is standard $k-\varepsilon$ model (Launder and Spalding 1974) which can be expressed as below:

$$\mu_t = \rho c_\mu \frac{k^2}{\varepsilon} \tag{2.7}$$

where

k = Turbulent kinetic energy (J/kg)

ε = Rate of dissipation of turbulent energy (J/kg•s)

c_μ = Empirically determined constant (c_μ =0.09)

Turbulent kinetic energy and rate of dissipation of turbulent energy are defined as below (Abbott and Basco, 1989):

$$k \equiv \frac{1}{2}\overline{u_i' u_i'} \tag{2.8}$$

$$\varepsilon \equiv -2\nu\overline{s_{ij} s_{ij}} \tag{2.9}$$

where

$$s_{ij} \equiv \frac{1}{2}\left(\frac{\partial u_i'}{\partial x_j} + \frac{\partial u_j'}{\partial x_i}\right) \tag{2.10}$$

u_i' is fluctuating velocity component.

The standard $k-\varepsilon$ model has been proven to be precise enough for fully developed turbulent flows which have great Reynolds number. However, in indoor air

environment, Reynolds number is relatively small. Thus, application of standard $k-\varepsilon$ model to indoor air flow simulation may lead to distinct computational error with regard to its overestimation to turbulent diffusivity. Therefore, modifications have been proposed to improve $k-\varepsilon$ model for low Reynolds number flows. Chen (1995) compared eight modified $k-\varepsilon$ models and pointed out that the Renormalisation Group (RNG) $k-\varepsilon$ model (Yokhot et al. 1992) performs best among all the eddy-viscosity models tested for mixed convection flow. Yuan et al. (1999) employed this model to predict indoor contaminant distribution in a displacement ventilated room.

In this study, we applied RNG $k-\varepsilon$ model to reach computational simulation for PDV and DV cases.

2.2.3 Discretisation technique

Discretisation divides computational domain into a number of small control volumes and grid points. Different grid topologies are possible; e.g. quadrilateral and triangular cells in 2D, and hexahedral, tetrahedral, pyramid, and wedge cells in 3D, as well as hybrid meshes containing quadrilateral and triangular cells or hexahedral, tetrahedral, pyramid, and wedge cells.

When the geometries of computational boundaries are complex or the range of flow length scales are large, unstructured meshes can be created with far fewer cells than structured meshes and thus less CPU time. This is because unstructured meshes allow cells to be clustered in certain regions of the flow domain, whereas structured meshes generally forces cells to be placed in regions where they are not needed. However, structured meshes permit a much larger aspect ratio than unstructured meshes. Because a

large aspect ratio in unstructured meshes will affect the skewness of the cell to some extend, and this may impede accuracy and convergence (Fluent 2001). In principle, structured meshes are more reliable to apply than unstructured meshes when the boundaries' geometries are simple.

Differential equations are integrated over control volumes and an interpolation schemes are needed for discretisation. A lot of schemes are available such as first order upwind scheme and second order schemes. Application of a certain scheme depends on the meshes generated in computational domain. Generally, first order scheme introduces noticeable numerical diffusion (also termed as false diffusion) under a convection dominated situation. High order scheme can help reduce the effects of numerical diffusion and present a better accuracy, but could lead to unstable solution.

2.2.4 Boundary conditions

In viscous flow, when fluid pass a wall type boundary used to bound fluid and regions, the fluid velocity in boundary layer decreases to zero on the boundary surface due to no-slip boundary condition. The high friction greatly affects flow pattern. The velocity and temperature gradient in boundary layer could turn sharply. Thus, we have to use very dense grid close to walls and this accounts for high demand of computer processing speed and memory.

Wall functions (Tennekes 1972) can be employed to determine surface friction. Standard wall functions divide boundary layer into two regions, viscous sub-layer and fully turbulent region.

$$u^+ = \frac{u}{u_\tau} \tag{2.11}$$

$$u^+ = y^+; \qquad 0 < y^+ < 11.225 \tag{2.12}$$

$$u^+ = \frac{1}{0.42}\ln(Ey^+); \qquad 30 < y^+ < 130 \tag{2.13}$$

where

u^+ = Dimensionless velocity

u = Velocity component in x direction (transversely to y direction) (m/s)

u_τ = Friction velocity (m/s)

y^+ = Normal-distance Reynolds number ($y^+ = \frac{\rho y u_\tau}{\mu}$, $u_\tau = \sqrt{\frac{\tau_w}{\rho}}$, y = Normal-distance to the wall)

E = Wall roughness constant. For smooth wall, $E = 9.81$ (Fluent 1996)

Reynolds' analogy between momentum and energy transport gives a similar logarithmic law for mean temperature. As in the law-of-the-wall for mean velocity, the law-of-the-wall for temperature can be determined with similar functions.

$$T^+ = \frac{T_s - T}{T_\tau} \tag{2.14}$$

$$T^+ = \sigma_H \left(u^+ + P(\mathrm{Pr}/\sigma_H)\right); \qquad y^+ > y_T^+ \tag{2.15}$$

$$T^+ = \mathrm{Pr} \cdot y^+; \qquad y^+ < y_T^+ \tag{2.16}$$

where

T^+ = Dimensionless temperature

y_T^+ = Non-dimensional thermal sublayer thickness ($y_T^+ = y^+ / \mathrm{Pr}$)

σ_H = Turbulent Prandtl number (0.85 at the wall)

Pr= Prandtl number

$P(\mathrm{Pr}/\sigma_H)$ = Constant which is a function of laminar and turbulent Prandtl number (Fluent 1996)

2.2.5 CFD validation

Despite CFD approach has become more precise in recent years, validation of computational simulations by experimental data remains necessary. Because the uncertainties derived from application of turbulent models and solver algorithms are almost unavoidable (Chen 1997, Baker et al. 1997).

A lot of experimental data are provided by other researchers but very few could be used to validate the simulation of specific PDV. Most existing studies are not delivered for PDV which could be considered as a combination of natural and forced convection. To improve the reliability of the CFD technique applied in this study, influence to air flow pattern of micro-environment around occupants from effect of multiple heat sources and obstacles has to be taken into account. Thus, in the next chapter, we developed a set of full-scale experiments regarding PDV and DV and will use the data to further validate the CFD model.

Chapter 3 Experiments and Results

3.1 Introduction

Experimental measurement, in principle, could provide the most practical and reliable information regarding temperature, velocity magnitude, contaminant concentrations and other parameters at specific experimental points. A lot of indoor experimental data are provided in the literature. For instance, Cheesewright et al. (1986) provided natural convection experimental data and Nielsen at al (1978) provided forced convection experimental data. However, not much of them can be used to validate the simulation results of PDV because they are either too simple or not delivered for PDV cases. Loomans (1998) conducted several full-scale PDV experiments to investigate thermal comfort through temperature distribution and air flow pattern. However, the contaminant concentration distribution was not considered in his experiments.

In this study, we conducted a set of full-scale chamber experiments to study the airflow, temperature and pollutant transport by PDV. Influence on air flow pattern, temperature and concentration distributions of the micro-environment around occupants from the effect of multiple heat sources and obstacles in the mockup room were also taken into account.

3.2 Chamber set-up

3.2.1 Chamber equipment

We conducted all the experiments using the Building Environment Simulation and Testing Facility, a state of the art installation at the Pennsylvania State University, Department of Architectural Engineering. The facility is designed for full scale thermal and air quality research. It consists of an environmental and a climatic chamber each with its own Heating, Ventilation and Air-Conditioning (HVAC) system. Another important aspect of the facility is its sophisticated measuring and data acquisition systems that are used to ascertain the energy consumption, air quality, and thermal comfort of different HVAC systems.

Figure 3.1 Photograph of the experimental facility at Pennsylvania State University

The facility is composed of two chambers, one is indoor environmental chamber and the other is outdoor climate chamber. The chambers' walls are constructed with R-30 insulation and coated with galvanized steel on both sides to protect against external influences. There is a partition wall with a sliding window which divides the climate and environmental chambers.

Each of the chambers has a separate Air Handling Unit (AHU) capable of simulating various environmental conditions. Both AHUs have a pre-filter and a High Efficiency Purification of Air (HEPA) filter which together provide 95% cleaning of outdoor air.

3.2.2 Chamber configuration

Environmental chamber

The environmental chamber was 6m x 3.9m x 2.35m in size and capable of simulating indoor air conditions, including air temperature, relative humidity, volume flow rate, and room air distribution.

Climate chamber

The climate chamber was 2.4m x 3.9m x 2.7m in size and capable of simulating a variety of outdoor weather conditions. The chamber can simulate cold dry winters as well as hot and humid summers. The controllable factors are air temperature, relative humidity, and wind pressure.

Model office room

A model office room was built within the environmental chamber to mimic PDV and DV respectively. The schematic of the model room is shown in Figures 3.2 and 3.3. The air supply inlet was located against the wall and outlet was placed in the center of the south part of the ceiling. For the PDV, one occupant and one computer were placed in front of the inlet as heat sources. The thermal manikin was seated in a chair. The upper part had about 6°backward inclination. A full description of the configuration and location of the different objects are given in Appendix A. For the DV, the occupant and computer were moved to the center of the room and the other boundary conditions remained the same in order to compare PDV and DV systems' performance.

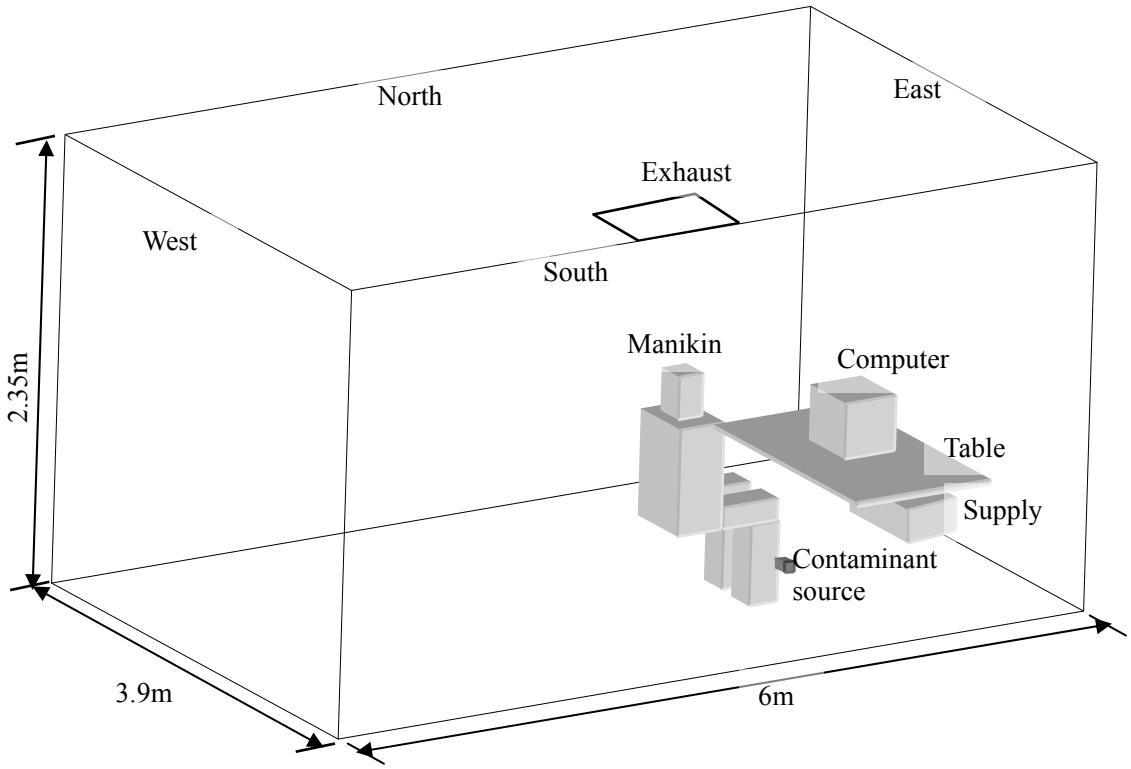

Figure 3.2 Schematic of the PDV test case

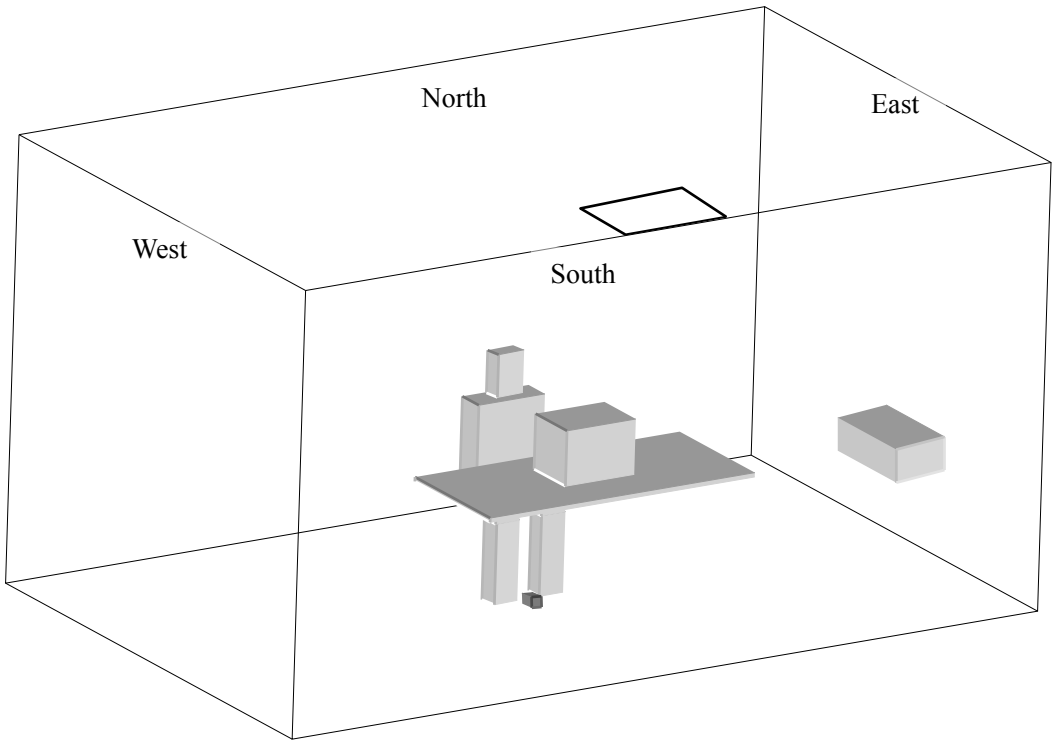

Figure 3.3 Schematic of the DV test case

3.2.3 Air handling and supply system

AHU control loops

Both chambers have the following three basic control schemes:

1. Constant air flow rate, constant supply temperature
2. Constant supply temperature, variable air volume (VAV) system
3. Variable supply temperature, constant flow rate

Control scheme one is intended for steady state measurements or for control of the supply air parameters when the load is regulated by fan coil or radiant systems.

Control schemes two and three are intended for measuring when variable loading is present. In a VAV system the partition window must be closed to prevent interaction between the air handling units and ensure stable control.

During the experiments, control scheme one was applied to supply air at constant flow rate and constant temperature.

Air supply and outlet

The supply unit is originally designed as a general displacement unit with apertures. It was partially sealed during the experiments and left 0.4 m (length) x 0.15 m (width) opening as a supply. The size of outlet was 0.34m x 0.14m and it was placed in the ceiling (Figures 3.2 and 3.3)

Supply flow rate

Average flow rate is 0.12 m^3/s (7.9 ACH) with fluctuation of 0.0025 m^3/s. During the experiments the flow rate was controlled by AHU control loops.

Supply temperature

Average supply temperature was 19°C with a fluctuation of ±0.5°C. It was also controlled by AHU control loops.

Contaminant source

SF_6 (0.1% SF_6 and 99.9% N_2) was used as the tracer gas which was released at a certain location through injection pipe as a point contaminant source. The mass flow rate of SF_6 injection was 8.03ml/min during the experiments.

3.2.4 Heat sources

Heat sources are employed to simulate the heat load in the office room. To emphasize the buoyancy effect around occupants, we limited the heat sources to one person and one computer.

Person

A seated thermal manikin (Figure 3.4) was used to represent the proportions of the human body on geometry and heat transfer process. The shape of this manikin has been simplified to a group of cubes which simulate head, chest and two legs. The height of manikin is 1.6m and surface area is 1.68m^2. Heating panels are dispensed inside of thermal manikin to generate heat of 76W.

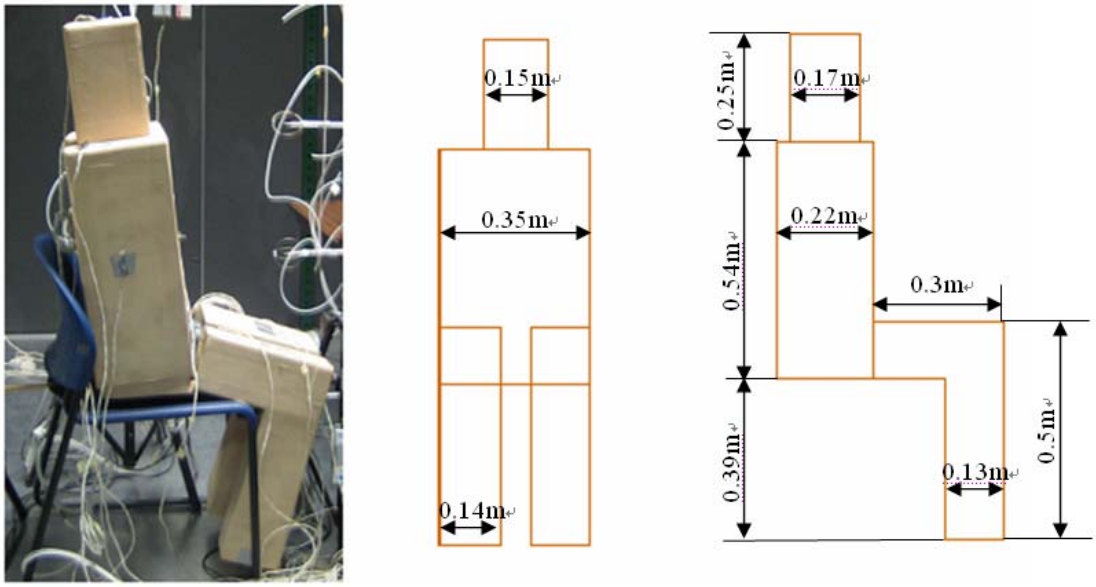

Figure 3.4 Thermal manikin in experiments and simulations

Computer

The computer is simulated by a 0.46m (length) x 0.32m (width) x 0.37m (height) chipboard box. The box was sealed on all surfaces and placed on the table in front of thermal manikin during the experiments. A 40W heat source (lamp) was placed in the middle of the box.

Photographs of environmental chamber configuration in PDV and DV experiments are shown in Figures 3.5 and 3.6.

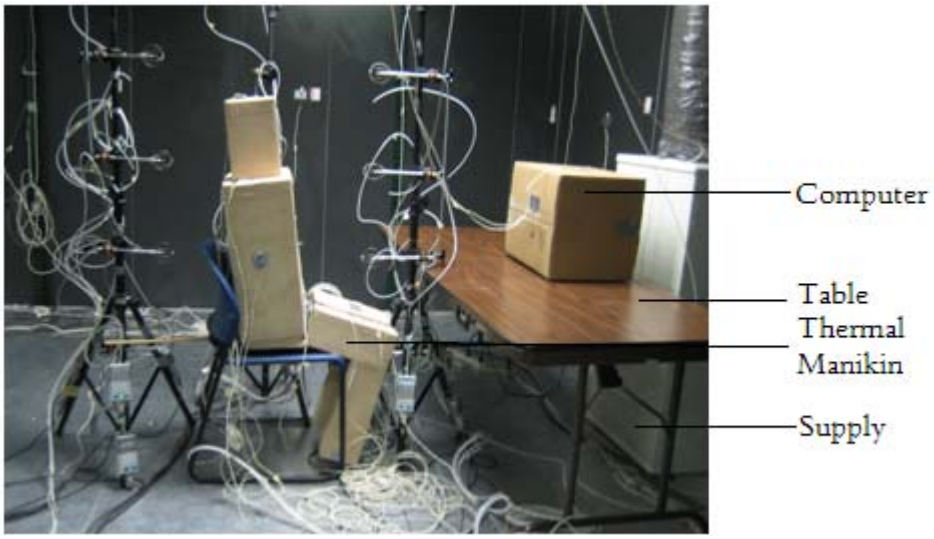

Figure 3.5 Configuration of environmental chamber in PDV experiments

Figure 3.6 Configuration of environmental chamber in DV experiment

3.3 Measurement equipment

The measuring equipment is divided into three main systems:

- Air velocity and temperature measurement system

- Surface temperature measurement system
- Tracer gas testing system

3.3.1 Air velocity and temperature measurement system

This system is based on omnidirectional thermo-anemometer sensors. It can be used to take air temperature and low air velocity measurements in rooms and inside air supply devices. The HT-400 measuring system consists of 24 omnidirectional probes (HT-412-0) with transducers (HT-428-0) connected to three measurement stations (HT-480). The system has the following technical properties:

Velocity Measurement Range:	0.05-5 m/s
Velocity Accuracy:	±0.02 m/s
Repeatability: 0.05-1 m/s	±1%
1-5 m/s	±3%
Temperature Range:	0-50°C
Temperature Accuracy:	0.2°C
Transducer Output:	Analog 0-20mA

This system provides the high level of accuracy and sensitivity recommended for low velocity measurements that are typical of indoor environments. The sensors provide a short response time which is critical in measuring velocity fluctuations. Each transducer is calibrated in a wind tunnel with laser doppler anemometry (LDA) reference. The software used for data acquisition compensates for the impact of barometric pressure on

velocity measurements and collects and stores data to computer disks. The data collected include mean velocity, root mean square (RMS) velocity, turbulence intensity, mean temperature and draught risk.

These 24 omnidirectional probes were placed on 5 poles, three of which located around manikin to detect temperature and velocity in micro-environment (Figure 3.5 and Figure 3.6) and the other two located in the other areas of the chamber.

3.3.2 Surface temperature measurement system

For precise measurement of temperatures at surfaces of manikin, computer and environmental chamber, a set of thermistors are provided. There are 56 Omega thermistors (series 44033) which are connected to four modules of InstruNet data acquisition systems, each supporting 8 channels. This allows for 32 points of dynamic measurement and 56 points of steady state measurement.

During experiments, thermistors were placed on ceiling, floor, walls (Figure 3.7) and surfaces of manikin and computer (Figure 3.5 and 3.6) to investigate surface temperature.

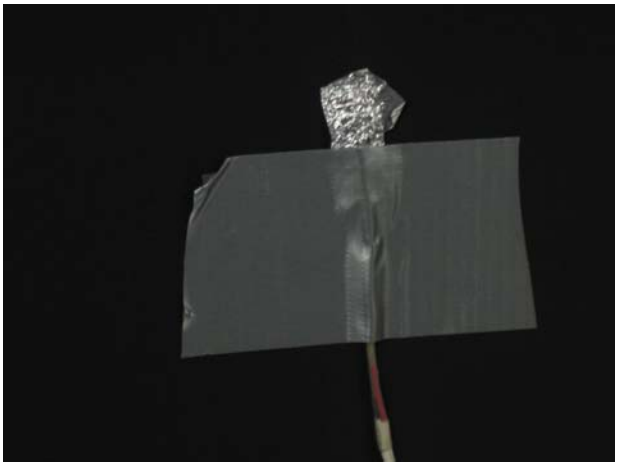

Figure 3.7 A thermistor attached to wall surfaces

3.3.3 Tracer gas testing system

The tracer gas testing system is a crucial component for the air quality measurement. The underlying concept of tracer gas testing is that a gaseous tracer can be dispersed in such a way that by following the movement of and measuring the concentration of tracer gas, one can determine airflow and contaminant movement in complex situations. The movement of a contaminant is investigated using a localized tracer injection and sampling for the presence of the tracer at various locations. SF_6 is used as the tracer gas since it is non-reactive, non-toxic, odorless, colorless, and it is detectable in small concentrations by a recognized measurement technique. The tracer gas system consists of three components:

- Instantaneous tracer gas injection system
- Continuous tracer gas injection system
- Sample collection and analysis system

During experiments, SF_6 was released continuously into certain points from a plastic pipe. Samples were collected through pipes placed along the poles which also carried omnidirectional probes (Figure 3.8). Samples were also collected at air supply inlet and outlet.

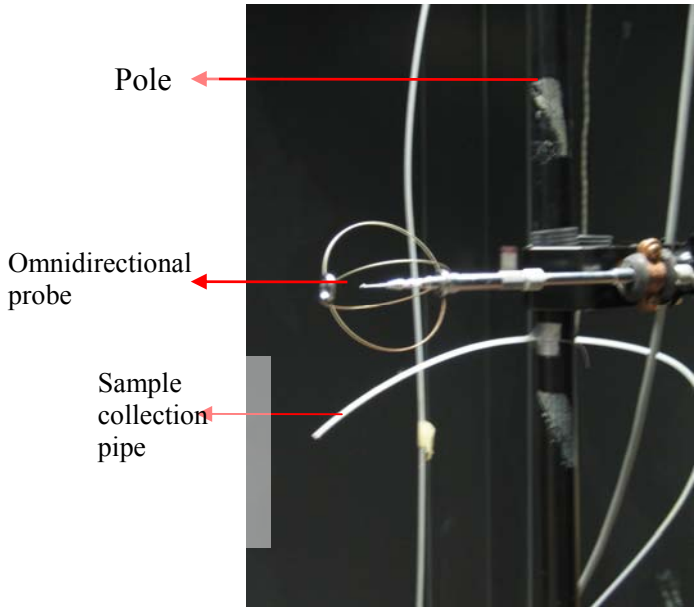

Figure 3.8 A pole carrying omnidirectional anemometer probes and SF_6 sampling pipes

Figure 3.9 SF_6 collection and analysis system

3.4 Measurement procedure

Measurement system takes charge of three measuring assignments as mentioned above, air temperature and velocity, surface temperature of objects and concentration of contaminant (SF_6). It takes around 24 hours to establish a stable temperature and contaminant concentration field.

To detect air temperature and velocity distributions in micro-environment around manikin and other parts of environmental chamber, 5 vertical poles were placed in the chamber. They carried 24 omnidirectional probes to measure air velocity and temperature. For each experiment, these 24 probes delivered data every 30 seconds in 30 minutes. The measuring process was repeated 2 hours after the first measurement.

To detect obtain surface temperature of walls and thermal objects, 32 thermistors were attached to the concerned surfaces. These thermistors delivered data every 30 seconds in 90 minutes. The measuring process was repeated 2 hours after the first measurement.

To detect the contaminant concentration indicated by SF_6, 25 sampling pipes were placed along the 5 poles which also carried omnidirectional probes and 2 pipes were also placed at air supply inlet and exhaust. Sample from each pipe was collected and analyzed once every 90 minutes. This measurement was repeated 3 times continuously.

3.5 Cases description and measurement equipments arrangement

In our study, we developed three PDV cases (Figure 3.2) and one DV case (Figure 3.3). All four cases have the same supply air parameters, contaminant injection rate and heat loads as discussed above.

The three PDV cases have the same setup of manikin, computer and table (Appendix A) but different location of contaminant source. In PDV case 1, the contaminant source was located 0.15m in front manikin's feet and 0.1m above floor; In PDV case 2, the contaminant source was located at the same x-position as case 1 but 1.1m above floor which is almost at the same height as manikin's mouth; And in PDV case 3, the contaminant source was located 0.15m at the back of manikin and 0.1m above floor (Figure 3.10).

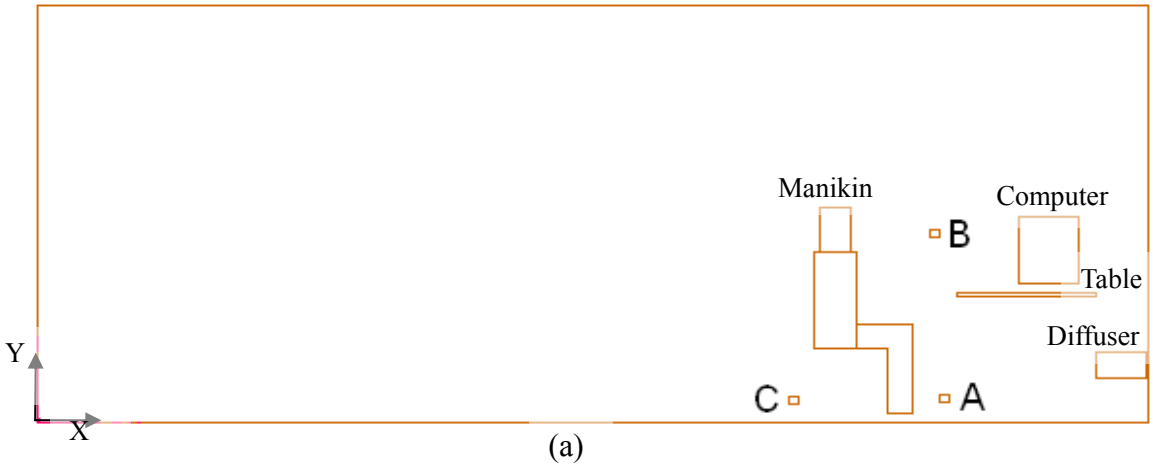

(a)

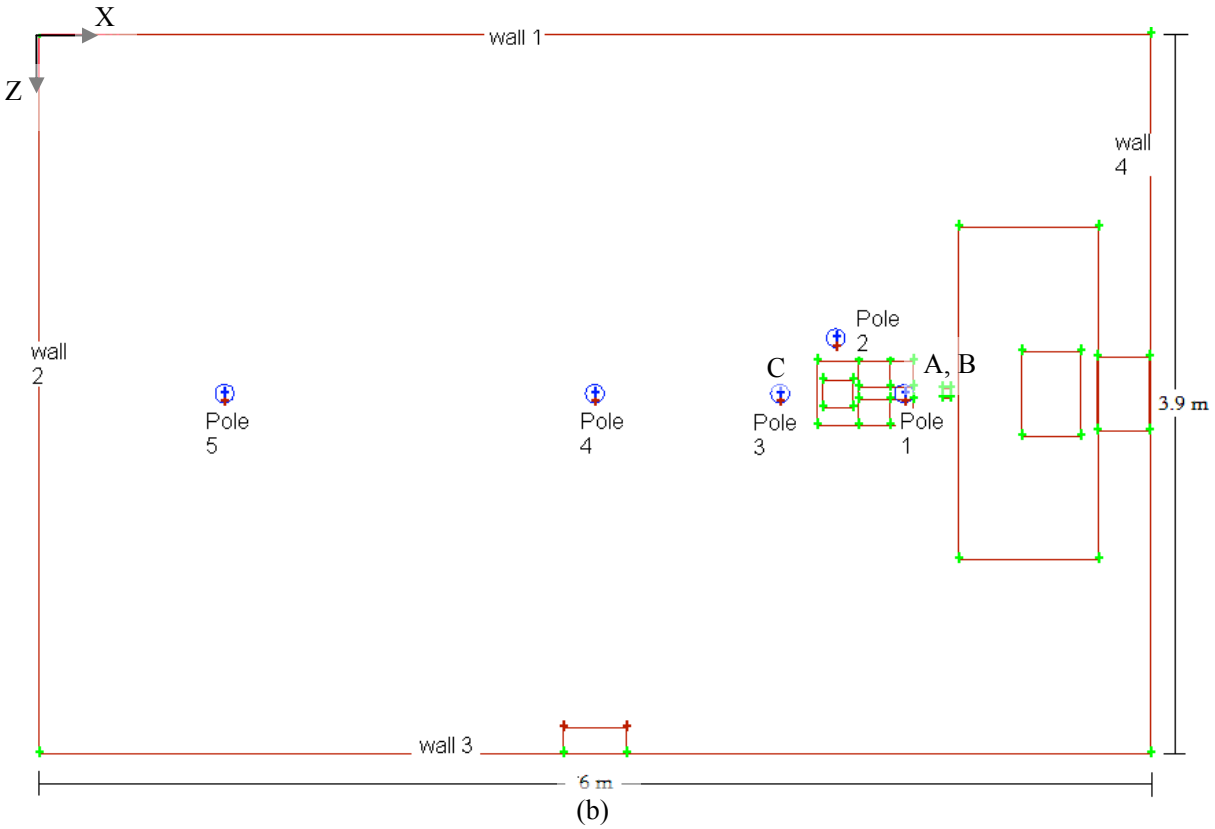

(b)

Figure 3.10 Layout of PDV test cases. A, B, C represent different contaminant source locations respectively. Pole 1- Pole 5 represent different measurement locations.

In DV case, manikin, computer and table were placed in the middle of the environmental chamber. And the contaminant source was placed 0.15m in front manikin's feet and 0.1m above floor which has the same distance to manikin as PDV case 1 (Figure 3.11).

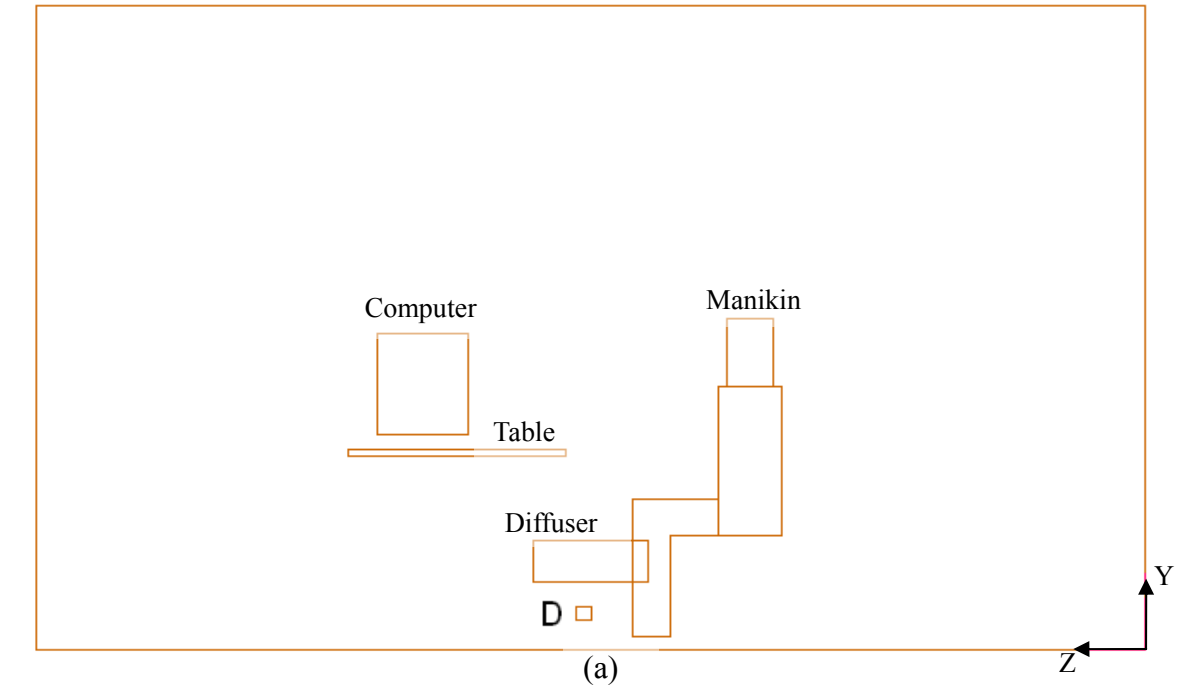

(a)

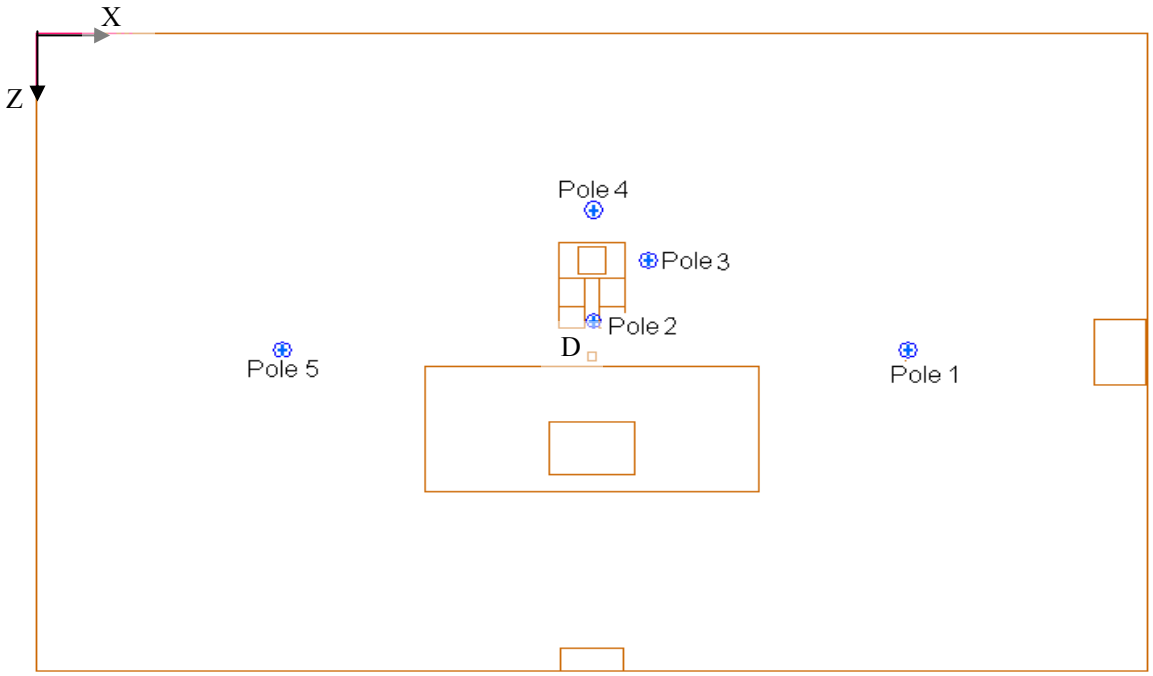

(b)

Figure 3.11 Layout of DV test case. D represents contaminant source location. Pole 1-Pole 5 represent different measurement locations.

Equipment arrangement

For each test case, 24 omnidirectional probes and 25 sampling pipes were fixed on five poles shown in Figures 3.10 and 3.11.

Probes and sampling pipes were placed at height from 0.4m to 1.8m which is within the range of occupied zone.

3.6 Results and discussion

Figure 3.12 shows measured velocity distribution for the three PDV and one DV cases respectively. All PDV cases have the same airflow pattern and temperature distribution owing to the only difference between these cases was the location of contaminant source.

For all cases, velocity in occupied zone was mainly under 0.1m/s, with small velocity variations (<0.05m) along the height. The largest variations happened at Pole 1 in PDV and Pole 2 in DV which were placed in the middle of manikin's legs. The largest velocity magnitude happened at 0.4m on Pole 1 in PDV, due to the short distance (0.7m) to inlet which supplied fresh air at 0.2m/s with fluctuation of 0.042m/s. The variation on Pole 2 in DV was mainly due to the buoyancy effect around manikin and so as the Pole 3 and Pole 4 which were placed respectively on the left and the back of the manikin.

Temperature was generally increased along height for both PDV and DV (Figure 3.13) due to the buoyancy effect of heat sources. The variations of temperature were less than 2℃ which meet the requirement for thermal comfort (The recommended level is 4□ by ASHRAE 1992 and ISO 1984). In PDV, due to the buoyancy effect around manikin, temperature gradient is relatively large at Pole 1 and Pole 2 which were located in the

middle of manikin's feet and on the left of manikin's chest. Whereas temperature gradient is relatively small at Pole 4 and Pole 5 which were 1~3m away from manikin. And the temperature gradient at Pole 3 (back of manikin) was smaller than Poles 1 and 2 and larger than Poles 4 and 5. For PDV, Figure 3.13 shows smooth temperature distribution at Poles 4 and 5. Temperature at Poles 1 and 2 increase greatly under the height of 1m which was the height of chest top and then changed slightly because the buoyancy effect prevailed under 1m (the majority heat was delivered from the chest and legs of manikin). For, the differences of variations among all 5 poles were not significant except Pole 1 which was located nearest to the inlet (1.3m) and thus had the lowest temperature in the lower part.

Contaminant concentration distribution is a great index to evaluate air quality. It depends on lots of parameters, such as the type of contaminant source, the type of ventilation, the position of inlet and outlet, the distance between the contaminant and heat objects, and etc. Results for the four cases, shown in Figure 3.14, are analyzed below.

In case 1, contaminant source was placed 0.15m in front of manikin's feet and 0.1m above floor. Concentration of contaminant at Pole 1, located in the middle of manikin's legs, increased along the height. It indicated that the contaminant was diluted greatly by supply air after generated from contaminant injection pipe. This happened if the contaminant source is placed close to the inlet, in this case, the distance between contaminant source and inlet was 0.7m. The concentration at Poles 3, 4 and 5 did not change much along height and it shows a well mixed contaminant distribution (concentration=1). The concentration on breathing level (around 1.1m high) was about 1

at Pole 1. It indicated when the contaminant is at lower and front location of the manikin, lower contaminant concentration at the breathing zone did not occur.

In case 2, the contaminant source was placed 0.15m in front of manikin's feet and at the same height of manikin's mouth (y=1.1m). The concentration generally increased along height at all five poles. Contaminant first dropped after being released from the injection pipe and then diluted by the plumes around manikin. The concentration on Poles 1, 2 and 3 which were close to the manikin was around 0.8 under the height of 1.2m (the height of head top). It demonstrated that the concentration in breathing zone is much better than a completely mixing case when the contaminant is at higher and front location of the manikin.

In case 3, the contaminant source was placed 0.15m at the back of manikin and 0.1m above floor. The concentration at Pole 1 increased till 1.2m high and then remained approximately the same at around 1.1. The concentration at Pole 2~ 4 which were located near to the contaminant source decreased till 1.2m high because contaminant was blown to the lower part of these poles once generated from the source. The concentration remained 0.8~1.1 above 1m which demonstrated it was no worse than a completely mixing case when the contaminant is at lower and back location of the manikin.

In case 4, manikin, computer and table were placed in the middle of the room to develop a DV case. The concentration at Pole 1 which located nearest to inlet (1.3m) increased along height as well as Pole 3 and 4 which located on the left and back of manikin. The concentration at Pole 2 & 5 decreased along height since the contaminant source were placed too near to Pole 2 (0.3m) and Pole 5 were placed too far to inlet to receive fresh air. Contaminant dropped once generated from the injection pipe and mixed

with air above floor. The average concentration was greater than 1 in breathing zone, thus, the concentration distribution is worse than completely mixing case when the contaminant is at lower and front location of the manikin.

Case 1 and case 4 both had contaminant source located in front of person's feet. They had the same boundary conditions except that case 1 applied PDV, whereas, case 4 applied DV. Figure 3.15(a) shows measured concentration on the pole which located in the middle of manikin's legs. Concentration of case 1 at this location increased along height under 1.4 m and then remained the same. On the contrary, concentration of case 4 at this location decreased along height under 1.4m and then remained the same. Because for PDV case 1, contaminant source was located too near to air supply inlet (about 0.7m), contaminant was first blown to the back of person after generated from source, then mixed with room air and flew back to occupied zone by air circulation. However, for DV, since contaminant source was located far away from air supply inlet (about 3m), contaminant was accumulated in front of person and then diffused to the other part of the room. Thus, PDV achieved lower contaminant concentration at breathing zone (0.8~1.2m high) than DV when contaminant source was located in front of person's feet.

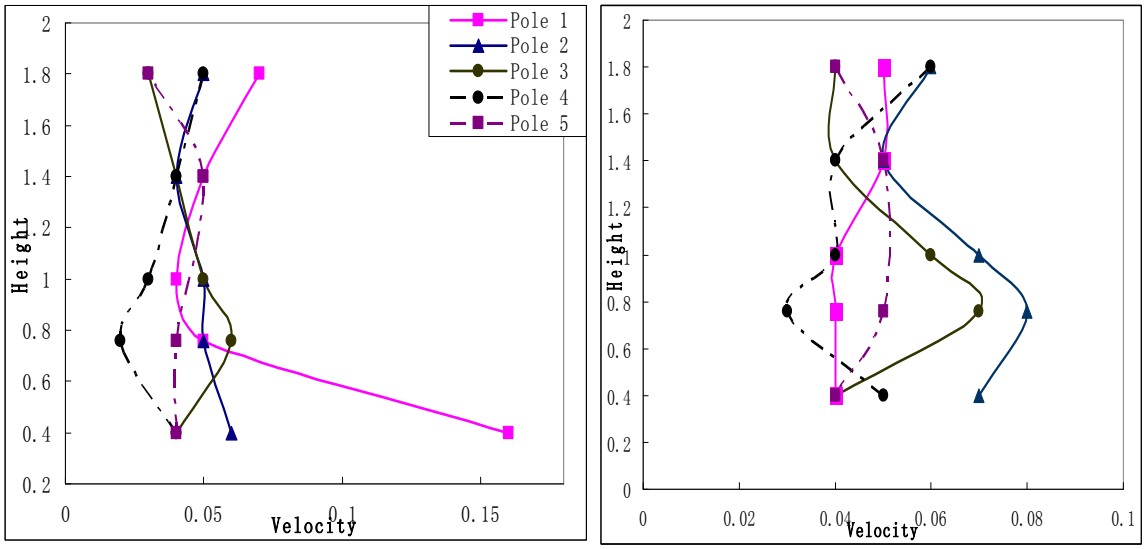

（a） PDV (b) DV

Figure 3.12 Measured velocity distributions for PDV and DV cases. See Figures 3.10 and 3.11 for pole locations

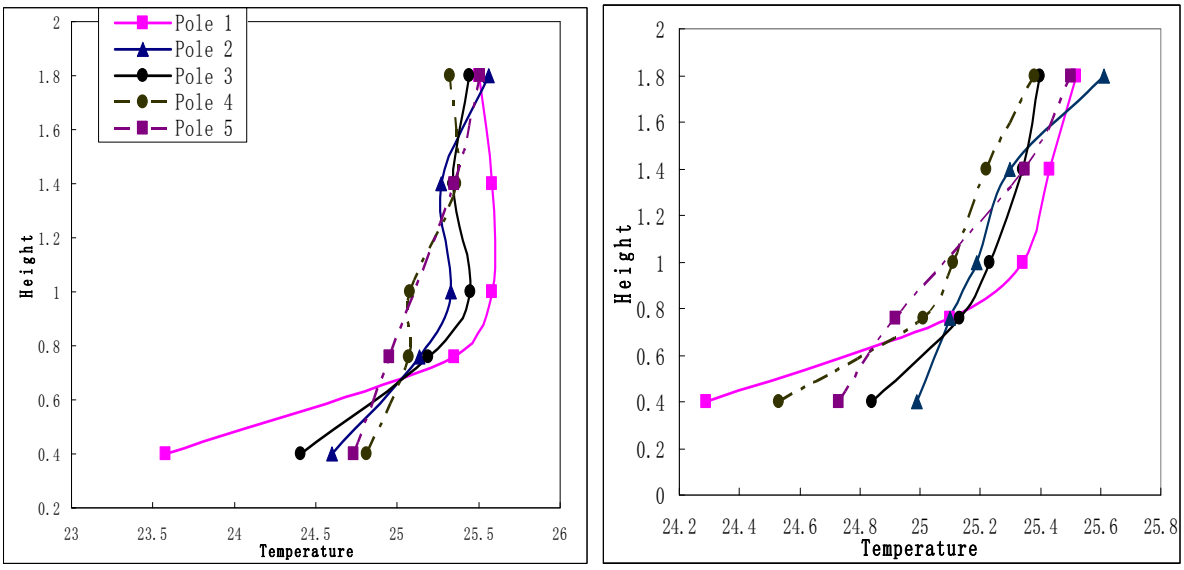

(a) PDV (b) DV

Figure 3.13 Measured temperature distributions for PDV and DV cases. See Figures 3.10 and 3.11 for pole locations

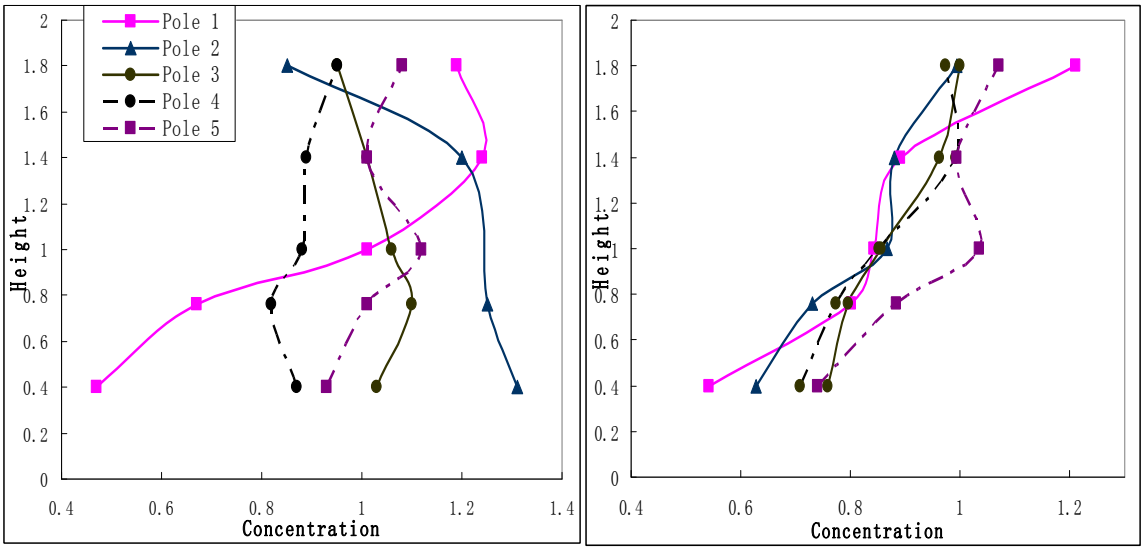

(a) PDV, contaminant source A (front, low) (b) PDV, contaminant source B (front, high)

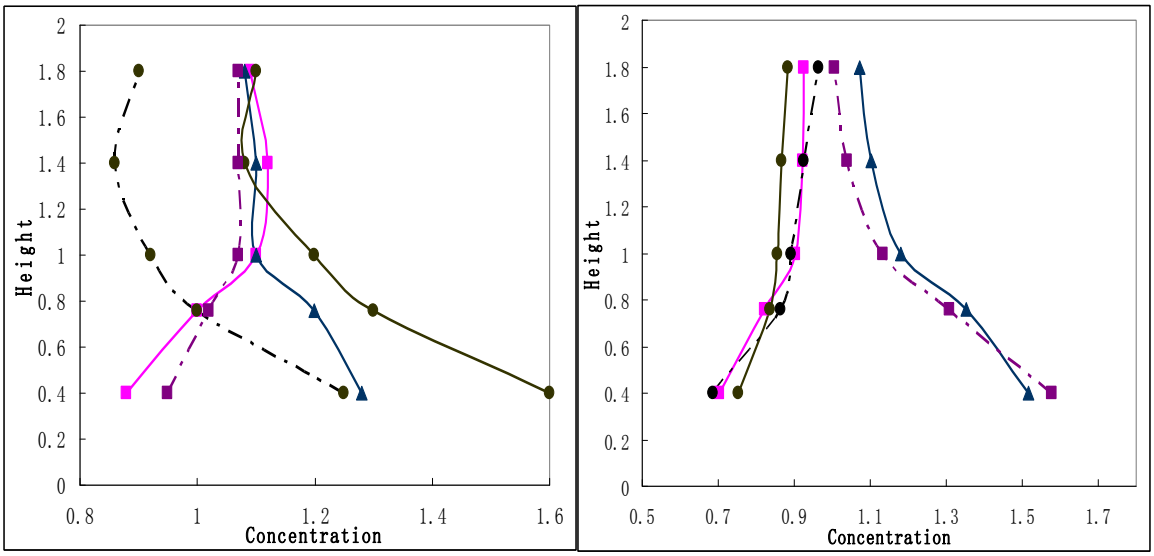

(c) PDV, contaminant source C (back, low) (d) DV, contaminant source D (front, low)

Figure 3.14 Measured concentration distributions for PDV and DV cases. Concentration has been normalized through dividing local concentration by average concentration at room exhaust. See Figures 3.10 and 3.11 for pole locations

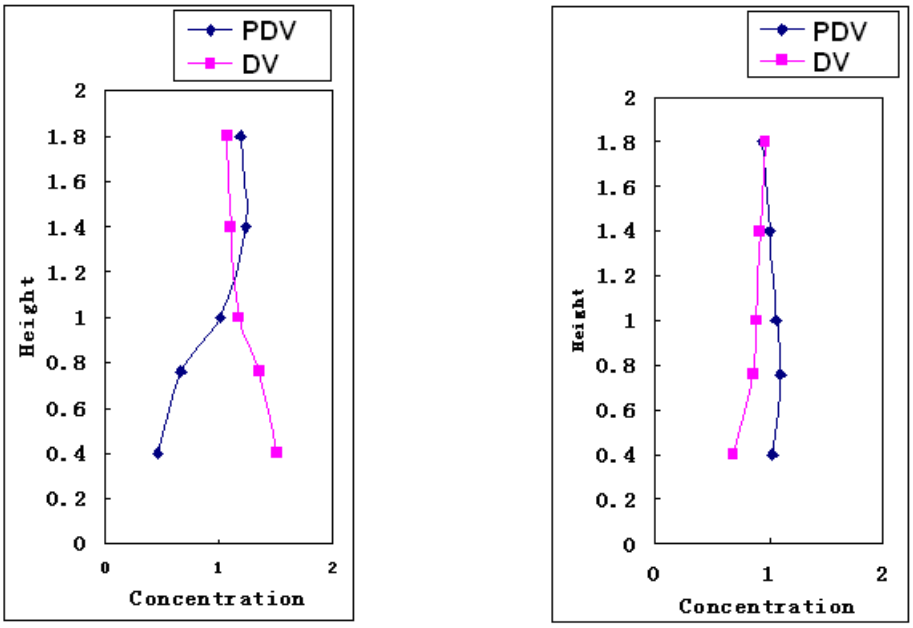

（a）Front of manikin (b) Back of manikin

Figure 3.15 Comparison of measured concentration distributions between PDV and DV cases

3.7 Conclusion

This chapter presents the experimental results for airflow, temperature and contaminant distributions in a mocked office room, using PDV and DV respectively. A point source was placed at different location of the room.

The results show that for PDV, when the contaminant is located at lower and front location of the manikin, lower contaminant concentration at the breathing zone did not occur. When the contaminant is at higher and front location of the manikin, concentration in breathing zone is much lower than a completely mixing case. When the contaminant is at lower and back location of the manikin, concentration in occupied zone

was no worse than a completely mixing case. For DV, when the contaminant is at lower and front location of the manikin, the concentration in occupied zone is worse than completely mixing case Whereas, further analysis of different scenarios need to be done in order to reach more conclusive results. These experimental data are also used for CFD validation in next chapter.

Chapter 4 Numerical Model Validation

This chapter presents the validation of computational fluid dynamic (CFD) model by comparing the simulation results with measurement data given in Chapter 3.

4.1 Introduction

CFD methods have been widely used in evaluating and predicting indoor environment recently. However, the reliability of CFD results has to be verified because of the application of discretisation technique and turbulent models during the calculation. Thus, CFD results can only be reliable once validated against experimental measurement.

As discussed in Chapter 2, RNG $k-\varepsilon$ model and structured meshes perform best when the Reynolds number of fluid is low and the boundary geometries are simple, we employed them to simulate all cases. Since the indoor heat source is a main force for the buoyancy flows, the Boussinesq approximation, which relates density change with temperature difference, is also employed. The simulations use the finite volume scheme and SIMPLE algorithm (Patankar, 1980) to solve discretized airflow equations.

Fluent 6.2 is a widely used commercial software to carry out CFD simulation results of any parameters in a computational domain including temperature distribution, fluid flow pattern, concentration distribution. It is used in this study.

4.2 Cases description

To validate PDV and DV simulations, we compare simulation results and experimental measurements for four ventilation cases described in Chapter 3 (Table 4.1).

Table 4.1 Descriptions of experimental cases

Cases descriptions	Supply method	Contaminant source's position
Case 1	PDV	In front of feet
Case 2	PDV	In front of mouth
Case 3	PDV	Behind back
Case 4	DV	In front of feet

Heat sources and contaminant sources are present in office the validation cases. The heat is transferred mainly by radiation and convection. However, the radiation is not calculated in the simulation. Instead, the radiation is taken into account by setting wall surface temperatures which are obtained from experiments (Table 4.2). The convection heat transfer is 76 W for manikin and 40 W for computer simulator. The emission rate of contaminant is 8.03ml/min. The ventilation rate is 43m^3/h and supply air temperature is 19℃.

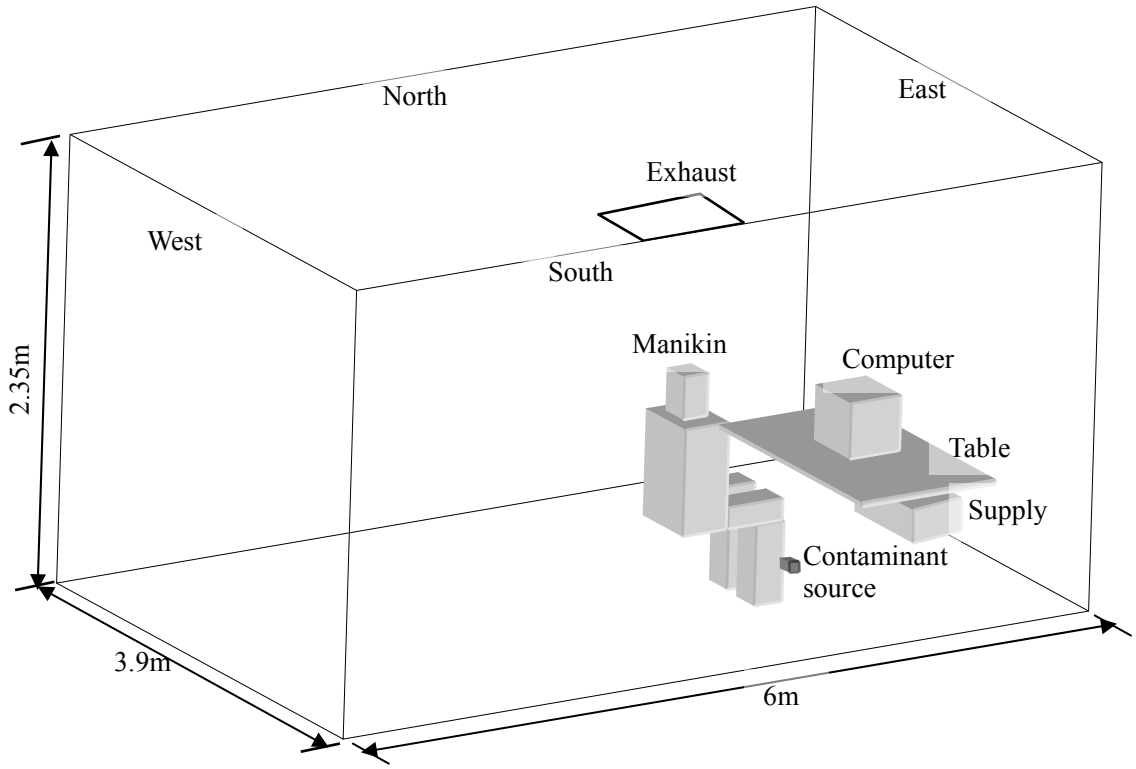

Figure 4.1 Schematic of the PDV test case

Table 4.2 Measured wall surface temperatures (°C)

Wall / Cases	North	South	West	East	Ceiling	Floor
Case 1	24.8	24.8	24.5	25	24.9	23.9
Case 2	24.7	24.7	24.4	24.9	24.8	23.8
Case 3	24.8	24.8	24.6	25.1	25	24
Case 4	24.6	24.6	24.6	24.4	24.7	23.7

4.3 Simulation results

To obtain precise simulation results, dense meshes are usually required. However, it will require high speed CPU capacity and long calculation time. To generate proper meshes which can not only bring us acceptable results but also save calculation time, we need to do mesh independence test. In this study, we generate two kinds of

meshes to simulate the PDV case 1 and then compare them with measurement results. They have the same structure but different densities which are 500 K meshes and 300 K meshes, respectively. The comparison of velocity, temperature and concentration distribution are shown in Figures 4.2-4.4. From these three figures, the difference of simulation results between 300 K meshes case and 500 K meshes case is acceptable. Thus, for other cases in this study, we can only apply 300 K meshes for simulation.

In case 1, the trends of velocity and temperature lines were the same at all five poles, but the variations at the points on Poles 1, 2 and 3 which are located around person were larger than Poles 4 and 5 located in the other zone in the room because of buoyancy effect around person (Figure 4.2).

The temperature (Figure 4.3) at Poles 1-3 greatly increased under the height of 1m which was the height of the top of person's chest and did not change much above 1m because 95% of heat source was released under 1m. The temperature difference under 1.2m (the height of seated person) at Pole 2 and 3 was about 3°C which meet the requirement of thermal comfort. But the temperature different was almost 4°C at Pole 1 because Pole 1 was placed in front of person and very near (0.7m) to the supply air whose temperature was 22°C. The experimental and simulation results matched perfectly at most of the points expect the 0.4m point at Pole 1. However, this difference (0.8°C) was acceptable because the temperature was very sensitive to the height of sensor since temperature changed 3.9°C under the height of 0.5m.

In case 4, the experimental and simulation results of airflow pattern matched well (Figure 4.7). The greatest difference was 0.04m/s which is acceptable. The velocity changed greater above 0.8m at Poles 2-4 which were located around person than Poles 1

and 5 because of the buoyancy effect of person's body. Similar to temperature distribution of PDV case 1, the temperature (Figure 4.8) at Poles 2-4 greatly increased under the height of 1m and did not change much above 1m. The experimental and simulation results of temperature distribution in DV matched perfectly well.

In case 1, the concentration (Figure 4.4) of contaminant at Pole 1 & 3, which located in the middle of person's legs and at the person's back, greatly increased and then decreased under 0.4m because the contaminant source was placed 0.15m in front of person's feet and 0.1m above floor. The contaminant was blown to the back of person by supply air after it was released. Thus, Pole 1 and 2 had the same trends of concentration lines. The concentration generally increased at Pole 2 which located on the left of person because contaminant can not directly reach the location of Pole 2. Thus, it had relatively clean air under 0.4m. The concentration above 0.8m did not change and was around 1. It indicated that the average concentration in breathing zone in this case was no higher than completely mixing ventilation. Both of the two simulation results match measurement results well enough

In case 2 (Figure 4.5), contaminant source was placed at height of person's mouth and outside the plume around person. The contaminant fell down after generated from the source and then joined the plume. Thus the concentration of contaminant was generally increased at all five poles and was below 1 especially at Pole 1. The concentration of breathing zone (about 1m height) was about 0.6 which indicated the performance of PDV in this case was much better than completely mixing ventilation. The experiment and simulation results perfectly matched in this case.

In case 3 (Figure 4.6), contaminant source was placed at the back of person and 0.1m above floor. The contaminant was blown to the back of the room, mixed with air and then brought back by flow of the air. Thus, the concentration at Pole 1 and 2 (located in the front and on the left of person) did not change a lot and was around 1 which indicated the average concentration in breathing zone in PDV case 3 was not higher than completely mixing ventilation. The contaminant concentration was much larger than 1 under the height of 0.5m at Pole 3, 4 & 5 because contaminant was blown directly to the position of these three poles. And the concentration was around 1 above 0.5m at these three poles which showed a perfectly mixing contaminant distribution.

In case 4 (Figure 4.9), contaminant source was placed 0.15m in front person's feet and 0.1m above floor which was the same relative position to person as case 1. The contaminant fell down to the floor once generated by the source, mixed with the air and then brought up by buoyancy effect. The concentration under 0.6m at Pole 2, which located in the middle of person's legs, was much larger than 1 because it was close to the contaminant source. The concentration generally increased at Pole 3 and 4 located on the left (on the side of supply air) and at the back of person. It indicated that the contaminant did not reach the position of these two poles directly. The average concentration of breathing zone was around 1. Thus, the average concentration in breathing zone in this case was not much different from PDV case 1.

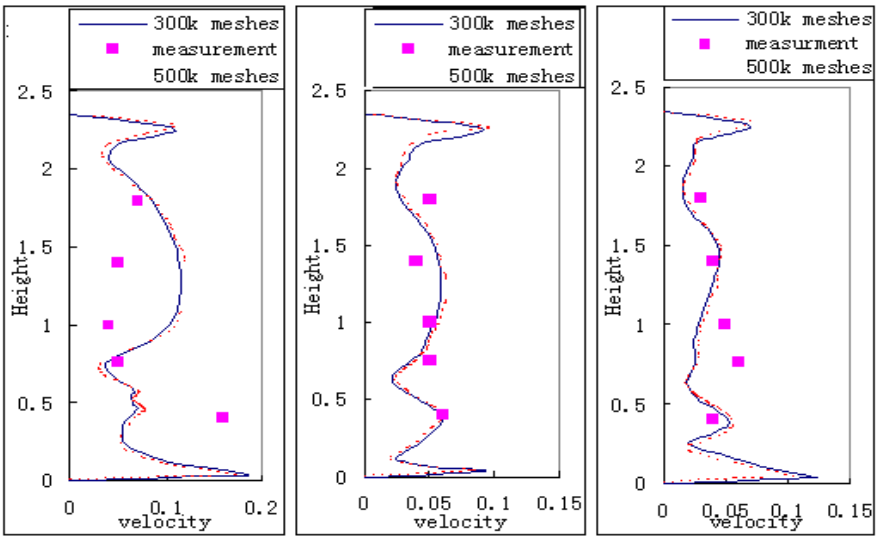

(a) Pole 1 (b) Pole 2 (c) Pole 3

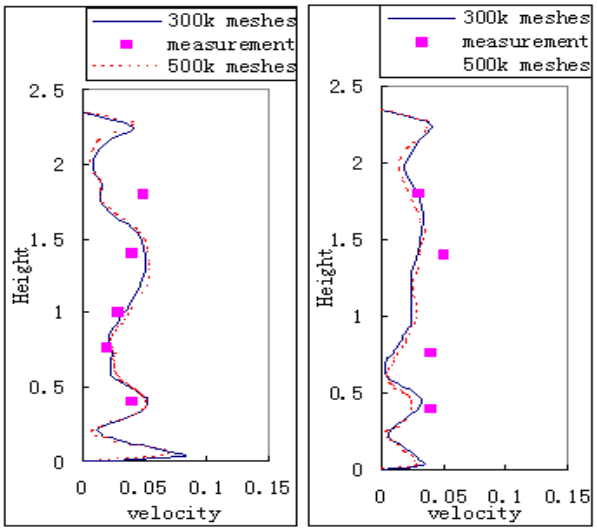

(d) Pole 4 (e) Pole 5

Figure 4.2 Comparison of velocity (m/s) distribution for case 1, PDV, contaminant source A (front, low). See Figure 3.10 for contaminant source and pole locations.

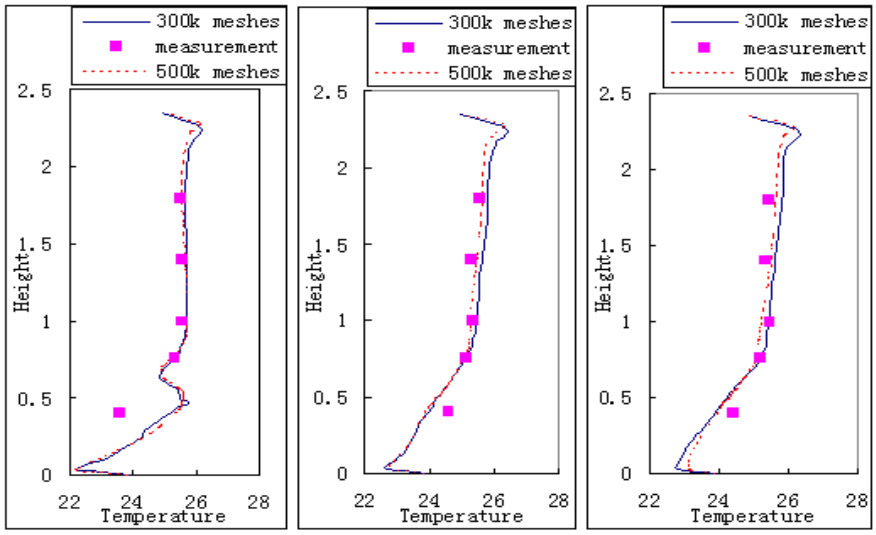

(a) Pole 1 (b) Pole 2 (c) Pole 3

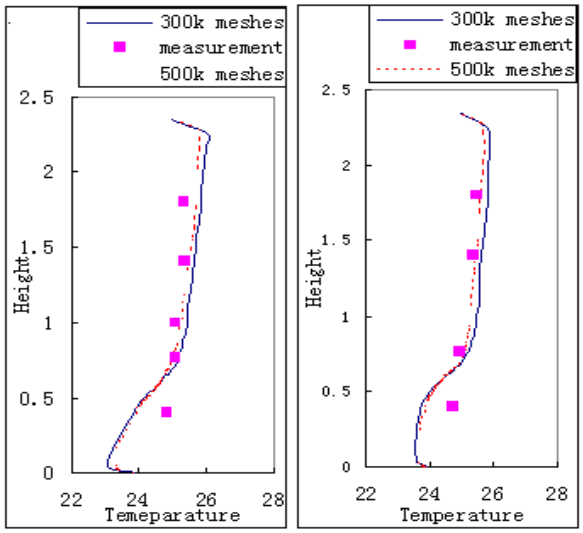

(d) Pole 4 (e) Pole 5

Figure 4.3 Comparison of temperature (°C) distribution for case 1, PDV, contaminant source A (front, low). See Figure 3.10 for contaminant source and pole locations.

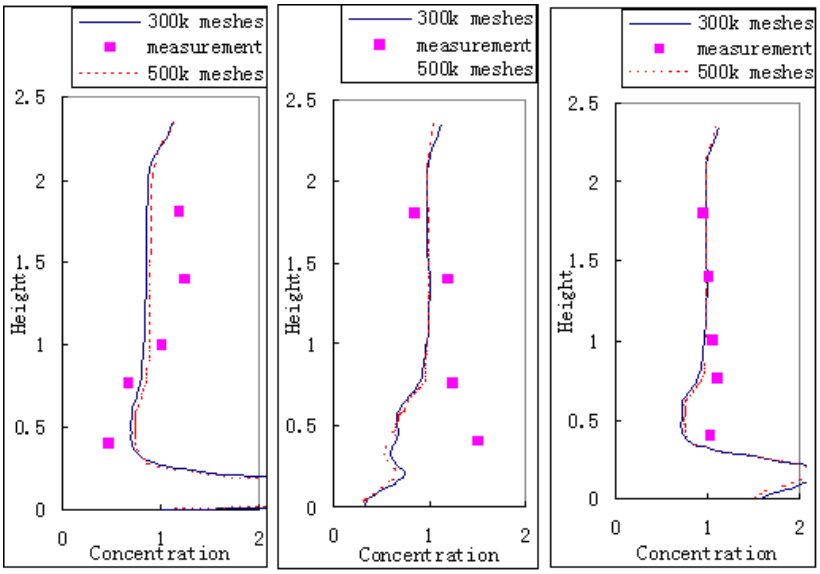

(a) Pole 1 (b) Pole 2 (c) Pole 3

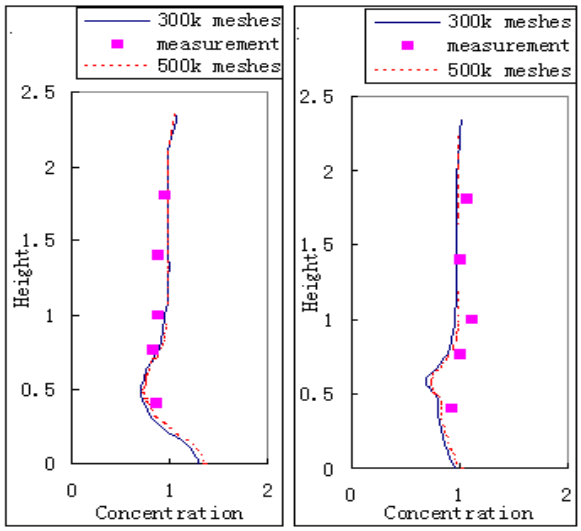

(d) Pole 4 (e) Pole 5

Figure 4.4 Comparison of contaminant distribution for case 1, PDV, contaminant source A (front, low). See Figure 3.10 for contaminant source and pole locations.

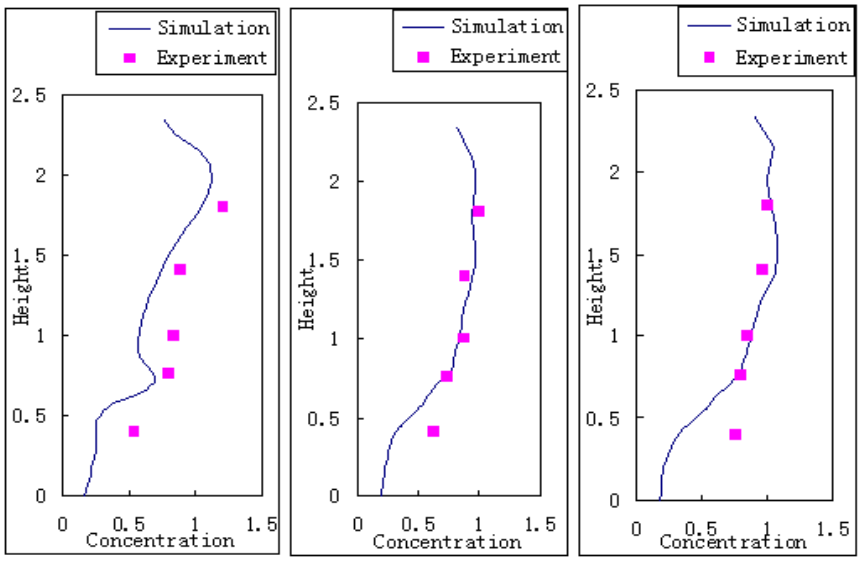

(a) Pole 1 (b) Pole 2 (c) Pole 3

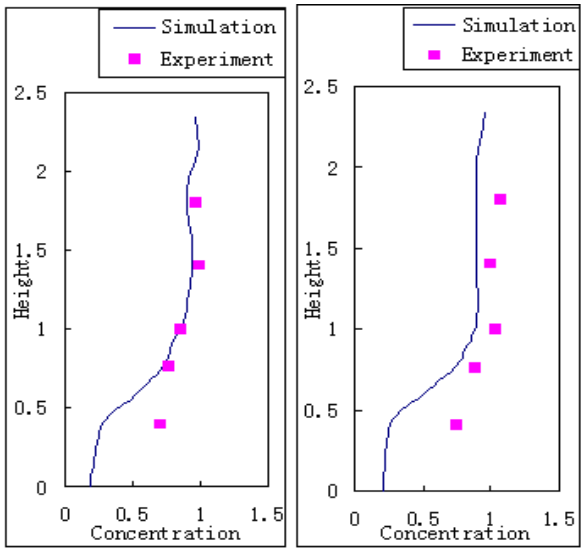

(d) Pole 4 (e) Pole 5

Figure 4.5 Comparison of contaminant distribution for case 2, PDV, contaminant source B (front, high). See Figure 3.10 for contaminant source and pole locations.

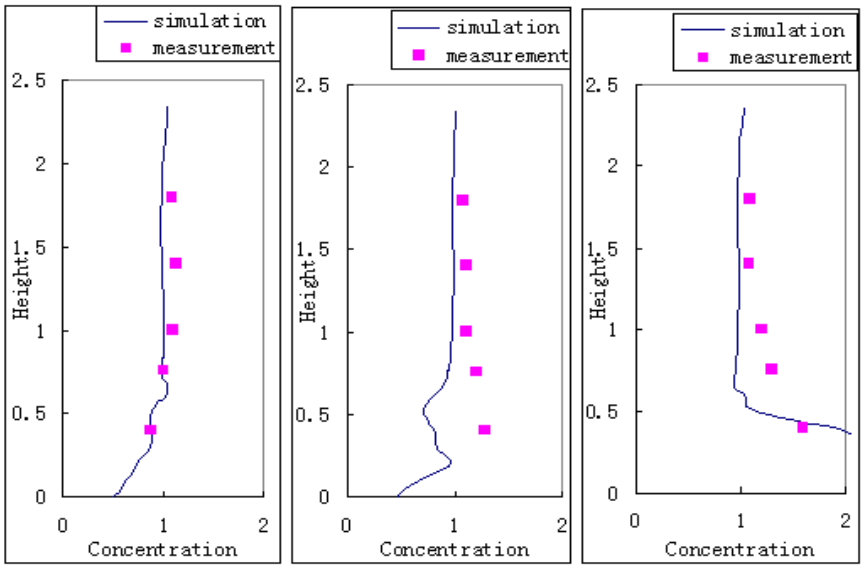

(a) Pole 1 (b) Pole 2 (c) Pole 3

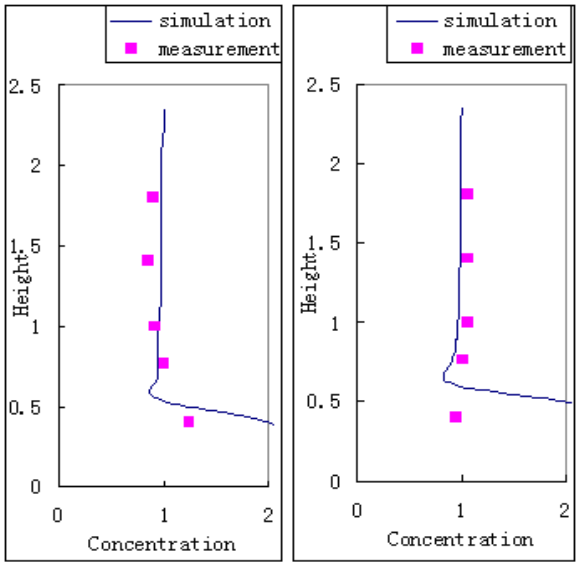

(d) Pole 4 (e) Pole 5

Figure 4.6 Comparison of contaminant distribution for case 3, PDV, contaminant source C (back, low). See Figure 3.10 for contaminant source and pole locations.

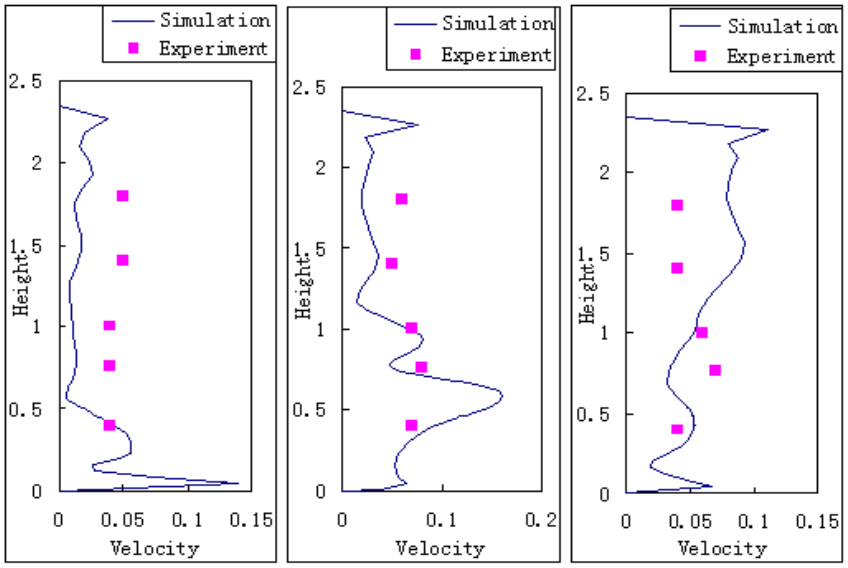

(a) Pole 1 (b) Pole 2 (c) Pole 3

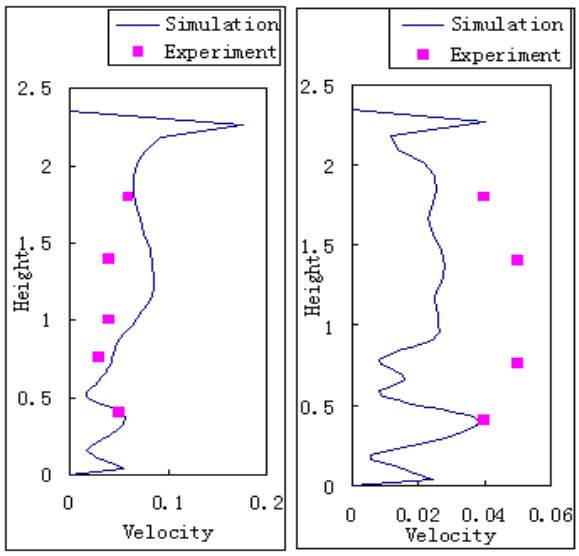

(d) Pole 4 (e) Pole 5

Figure 4.7 Comparison of velocity distribution for case 4, DV, contaminant source D (front, low). See Figure 3.11 for contaminant source and pole locations.

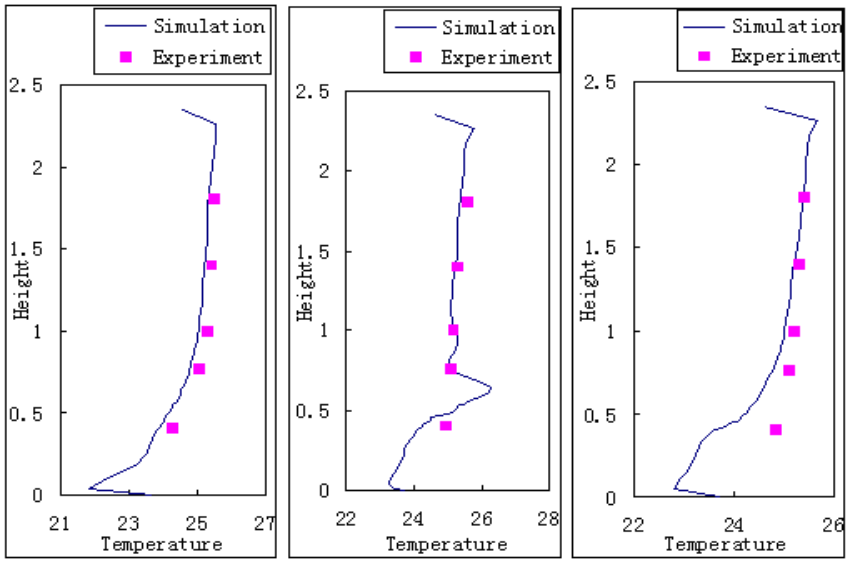

(a) Pole 1 (b) Pole 2 (c) Pole 3

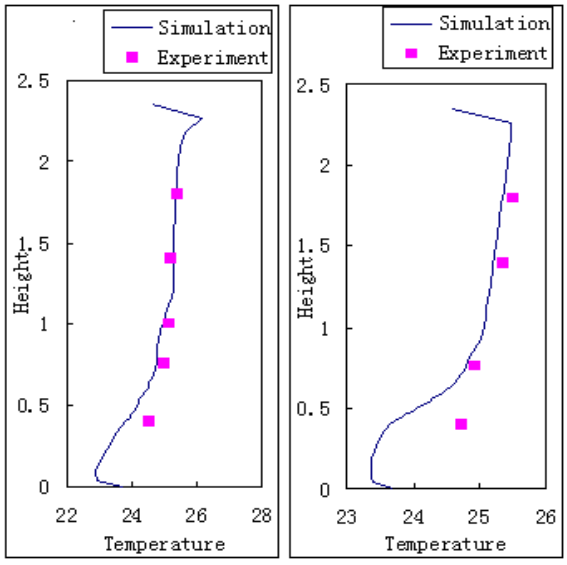

(d) Pole 4 (e) Pole 5

Figure 4.8 Comparison of temperature distribution for case 4, DV, contaminant source D (front, low). See Figure 3.11 for contaminant source and pole locations.

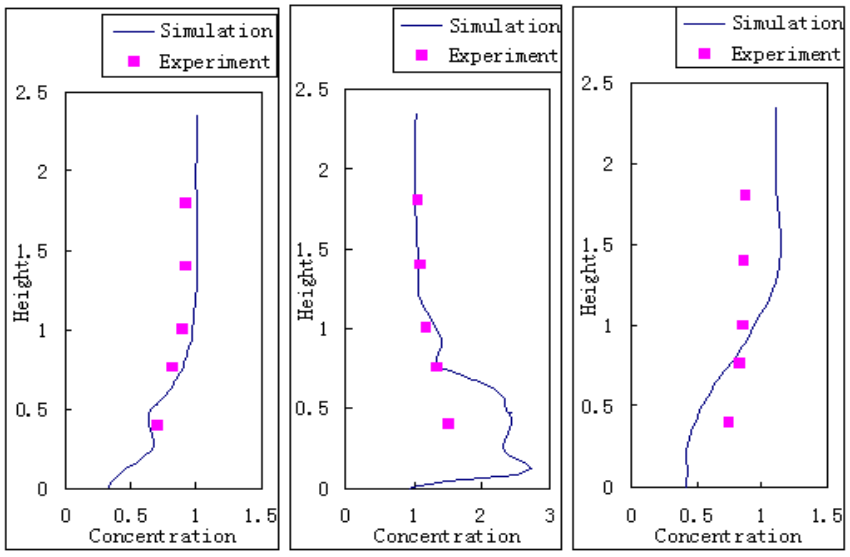

(a) Pole 1 (b) Pole 2 (c) Pole 3

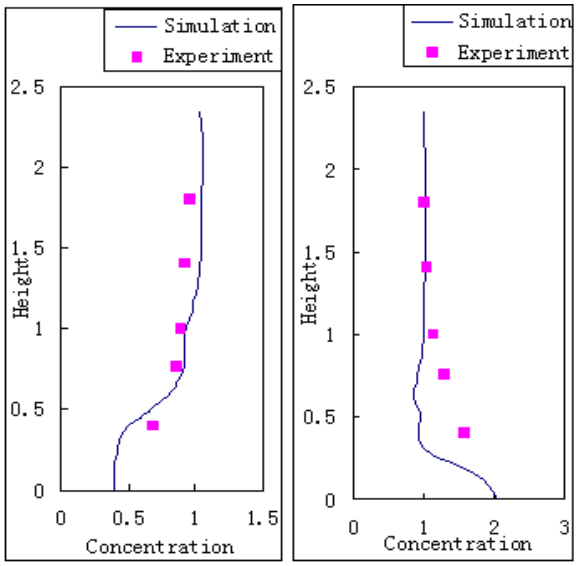

(d) Pole 4 (e) Pole 5

Figure 4.9 Comparison of contaminant distribution for case 4, DV, contaminant source D (front, low). See Figure 3.11 for contaminant source and pole locations.

4.4 Discussion of results

The experimental and simulation results generally match for these four cases as discussed above. The existing deviations between measurement and simulation result are due to unavoidable errors in both measurement and simulation of the complex boundaries and indoor conditions.

Chapter 5 Further Evaluation of PDV by CFD Modeling

5.1 Introduction

This chapter will present six simulation cases with the validated CFD model described in Chapter 4 and evaluate PDV through analyzing bypass factor, and local average contaminant concentration around person.

5.2 Cases description

To further evaluate PDV system, we designed six cases based on the three PDV cases in Chapter 3 but with certain changes of boundary conditions (Table 5.1).

Table 5.1 Cases description

Case description	Supply method	Direction of supply air	Contaminant source type and position	Distance between person and diffuser	High panels around person
Case 1	PDV	Horizontal	Point, in front of feet	1m	No
Case 2	PDV	Horizontal	Point, in front of mouth	1m	No
Case 3	PDV	Horizontal	Point, behind back	1m	No
Case 4	DV	Horizontal	Point, in front of feet	1m	No
Case A	PDV	Horizontal	Point, in front of feet	0.6m	No
Case B	PDV	Horizontal	Area, floor	1m	No
Case C	PDV	45°upward	Point, in front of feet	1m	No
Case D	PDV	Horizontal	Area, floor	1m	Yes
Case E	PDV	Horizontal	Point, outside high panels	1m	Yes
Case F	Floor supply	Vertical	Area, floor	1m	No

Since there was a measuring pole placed in the middle of manikin's legs, the distance between manikin and table was relatively large and thus the distance between manikin and air supply diffuser was large (1m) in experiments and validation simulations. In Case A, the distance between person and air supply diffuser was shortened to 0.6m. In Case B, we had an area contaminant source on the entire floor to further test PDV performance. In Case C, we adjust air supply's direction 45°up to find out if the fresh air could reach person directly in this way. In Case D, we used the same model configurations and boundary conditions as Case B but added high panels around person to block fresh air from traveling to the rest of the room. These high panels form an enclosed space around the person (Figure 5.2). In Case E (Figure 5.1), we put point source outside high panels to investigate if contaminant concentration near the person could be lower. And in Case F, we used the same model configurations and boundary conditions as Case B but placed the vertical diffuser on the floor to form a floor supply (vertical).

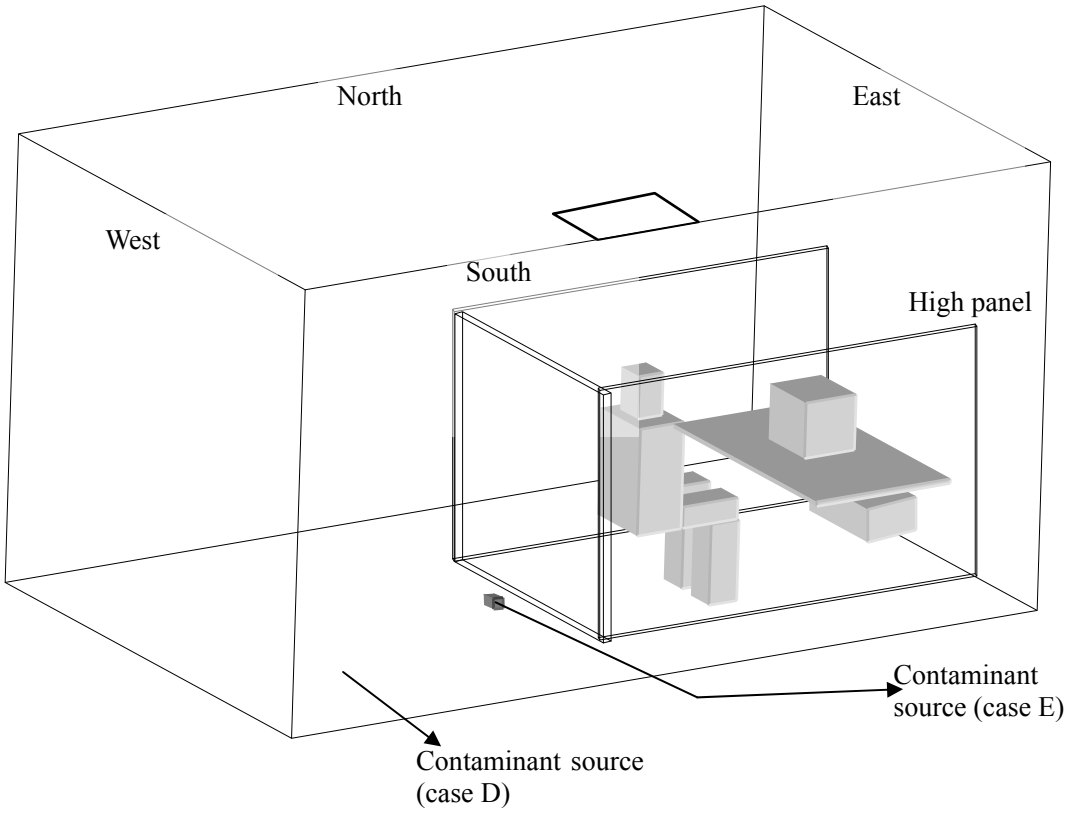

Figure 5.1 Adding high panels around person (case D and E)

Figure 5.2 Pictures of high panels in office room

5.3 Simulation results and analysis

In this part, we apply two index, ventilation bypass factor and local average concentration, to evaluate PDV performance in aspects of air flow pattern and contaminant concentration around person.

5.3.1 Ventilation bypass factor and analysis

Concept of ventilation bypass factor

Ventilation bypass factor (marked as *S*), which was proposed in ASHRAE Standard 62-1999 (ASHRAE 1999), is a straightforward indicator describing the fraction of the supply air that bypasses the occupied zone of a ventilated room.

$$S = 1 - \frac{Vsz}{Vs} \tag{2.17}$$

where

V_S is the total amount of supply air flow rate sent into the room

V_{SZ} is the amount of supply air flow rate that reach the occupied zone.

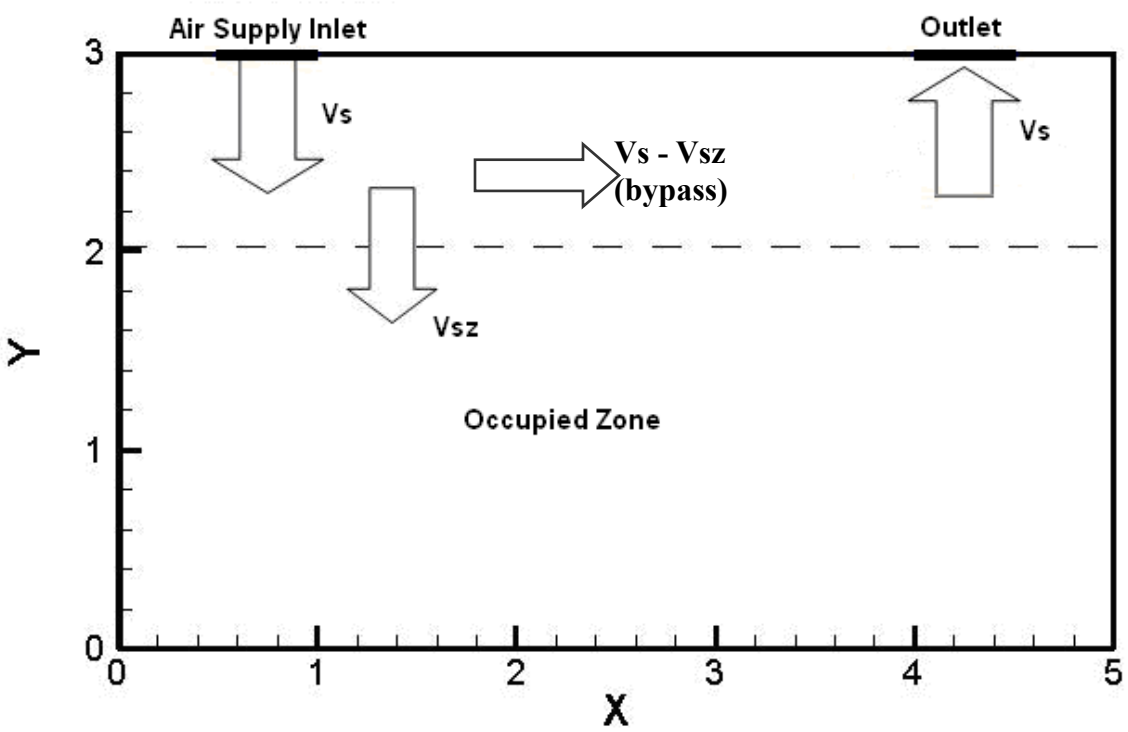

Figure 5.3 Two-dimensional schematic showing flow entering the occupied zone (Vsz) and bypass flow (Vs-Vsz)

Bypass factor (*S*) provides a numerical method to reflect the stratification of supply air and estimate how much supply air is not used to dilute the contaminant in concerned zones of a room.

Since *S* represents the characteristics of a systems, such as the configuration of room, the location of inlet and outlet, the air flow rate of supply air, the arrangement and area of concerned zones. Therefore it's unlikely to estimate *S* of a certain system by formula. Liu et al. (2006) employed CFD method to quantitatively estimate *S* by releasing hypothetical fine particles, which have small inertia that could be regarded as moving completely with air, at air supply inlet in order to represent the air path lines which could be tracked down by simulation method. And *S* is expressed by stating the percentage of the particles that bypass concerned zones.

Application and analysis of bypass factor

In our study, we applied bypass factor to investigate the fraction of supply that bypasses the zone around person's upper body by releasing 240 particles on the surface of air inlet and tracking down each particle to find out if they reached the certain zone or not (Figure 5.4). This zone consisted of 5 boundaries and the vertical four boundaries of which were 0.2m away from person's body. Since a large amount of supply air passed through person's legs to the rest zone of the room and this amount of supply air cannot count as contribution to the plume, the horizontal boundary of the selected zone was the same height as person's legs' top surfaces.

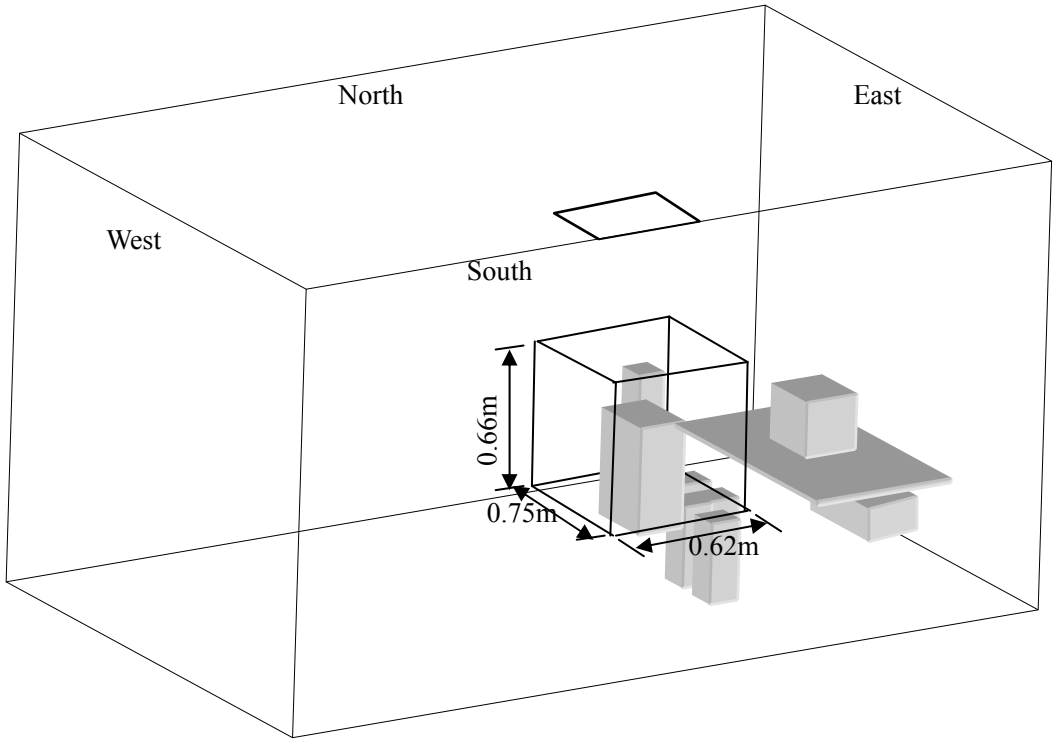

Figure 5.4 Range of the zone around person's upper body

Since ventilation bypass factor is an index that indicates the fraction of supply air that bypass the certain zone, this factor is only related to the air flow pattern but not concentration distribution. Cases 1, 2, 3 and B shared the same air flow pattern, and Cases D and E also shared the same air flow pattern, so they have the same bypass factor.

Table 5.2 Ventilation bypass factors (%) in each case

Boundaries / Cases	A1 below	A2 back	A3 front	A4 left	A5 right	Total ($\sum_{i=1}^{5} Ai$)	S (S=1-$\sum_{i=1}^{5} Ai$)
Case 1	16.7	10.4	20.8	10.8	5.0	63.7	36.3
Case 2	16.7	10.4	20.8	10.8	5.0	63.7	36.3
Case 3	16.7	10.4	20.8	10.8	5.0	63.7	36.3
Case 4	20.4	12.1	20.0	8.3	2.5	63.3	36.7
Case A	18.8	17.9	7.1	17.5	2.5	63.8	36.2
Case B	16.7	10.4	20.8	10.8	5.0	63.7	36.3
Case C	38.3	12.9	15.8	5.0	2.5	74.5	25.5
Case D	50.8	6.3	16.7	7.9	9.6	91.3	8.7
Case E	50.8	6.3	16.7	7.9	9.6	91.3	8.7
Case F	23.3	5.8	17.5	3.8	2.1	52.5	47.5

In PDV Case 1, 2, 3 and B, 63.7% of supply air reached the selected zone (Table 5.2), and 36.3% of supply air bypassed the zone. In DV Case 4, *S* did not have much change, 63.3% of supply air reached the selected zone and that means the PDV Case 1, 2, 3 and B did not have much difference from DV case at aspect of air flow pattern around person's micro-environment. This is because in PDV cases, supply air falls down to the floor after generated from diffuser due to the low flow rate of supply air. Since the buoyancy effect of person's legs is too small to attract the air, supply air flows through person's legs, travels around floor and mixes with room air, then flows back to join the

plume started from person's waist (Figure 5.5). Thus, air flow pattern around person in PDV has not much difference from DV.

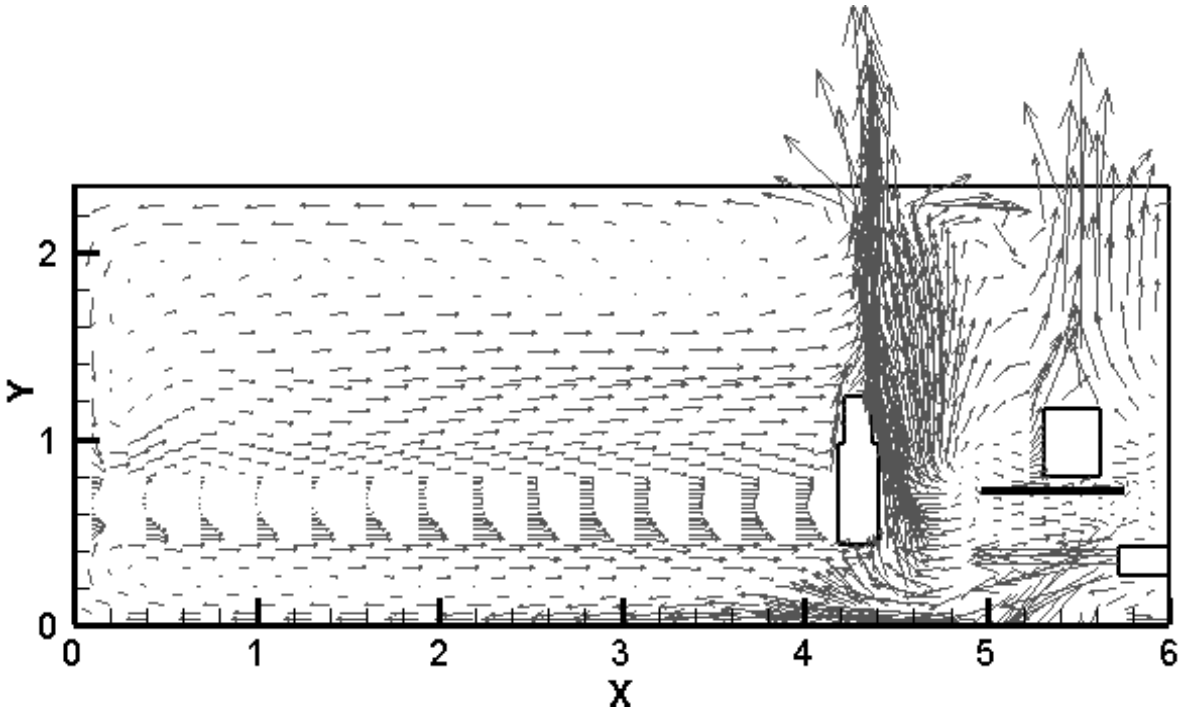

Figure 5.5 Air flow pattern in basic equipped PDV (cases 1-3)

In Case A, we move person 0.4m towards air inlet, and the *S* did not change a lot (36.2%). It indicates that decreasing the distance between person and diffuser cannot make supply air join the plume directly after generated from diffuser, therefore, cannot affect much to bypass factor.

In Case C, we adjusted the direction of supply air to 45°upward and *S* distinctly decreased. 74.5% of supply air passed through selected zone and the increase came mainly from the below boundary which means adjusting the direction of supply air is more effective than decreasing the distance between person and inlet in improving the air flow pattern around person.

In Case D & E, we added high panels around person, and *S* greatly decreased. 91.3% of supply air passed through selected zone and the increase came mainly from the below boundary. In these two cases, supply air still flows through person's legs after falls down from diffuser, but cannot travels far away from person owing to the limitations from high panels. It rises from floor when reaching the panels and flows back to join the plume started from person's waist (Figure 5.6). The low *S* indicated that adding high panels around person was the most effective method to improve air flow pattern around person.

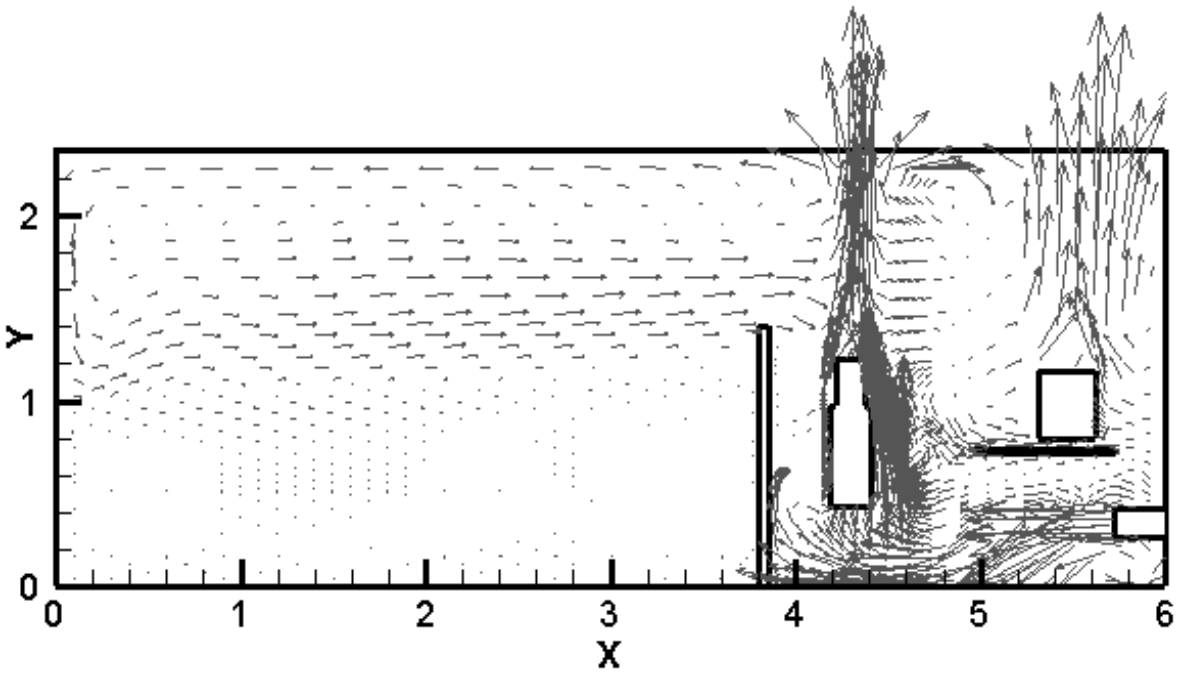

Figure 5.6 Air flow pattern in PDV with high panels

In case F, we applied floor supply, only 52.5% of supply air passed through selected zone. That means more supply air bypassed the zone in floor supply ventilation comparing to PDV and DV. That is because in floor supply ventilation, supply air falls down to the floor after generated from diffuser and then diffused around. Thus, only half

of supply air flew towards occupant directly; the other half flew away from occupant and then traveled around the floor.

The results show that the most effective way to decrease *S* (which means to increase the amount of supply air that passes through selected zone) is adding panels around occupant. Adjusting direction of supply air is also helpful.

5.3.2 Local average concentration and analysis

Local average concentration is another important index to evaluate the air quality in micro-environment around person and is also very difficult to predict because of the sensibility of the position of contaminant source. To investigate the average contaminant concentration in breathing zone, we defined a sphere zone which had radius of 0.3m (Figure 5.7). Then we calculated the average concentration in this zone and normalized this value by dividing the average concentration of outlet. The results of local average concentration are shown in Table 5.3.

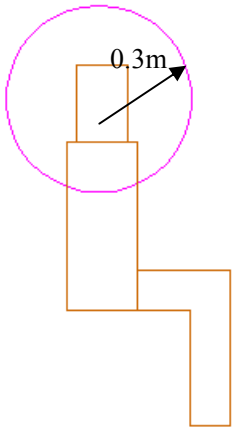

Figure 5.7 Range of breathing zone

Table 5.3 Local average contaminant concentrations in each case

Cases	Normalized average concentration
Case 1(source: in front of feet + PDV)	1.02
Case 2(source: in front of mouth + PDV)	0.75
Case 3(source: behind back + PDV)	1.03
Case 4(source: in front of feet + DV)	0.96
Case A(move case 1's person and source forward + PDV)	1.01
Case B(source: floor + PDV)	1.03
Case C(adjust case 1's air supply direction 45°up)	1.02
Case D(Case B + high panels)	0.99
Case E(source: behind high panels +PDV)	0.57
Case F(source: floor + floor supply)	1.00

From the local average concentration listed in Table 5.3, we find that the performance of basic equipped PDV had no much difference from or better than a completely mixing case or DV in these conditions. In case 1, contaminant was blown through person's legs after generated and mixed with room air, then reached breathing zone (Figure 5.8a). The average concentration in breathing zone at PDV case 1 (1.02) was not much different from completely mixing case (concentration=1).

In case 2, although the contaminant source was placed 0.55m in front of person's mouth, local concentration was relatively low because the contaminant fell down once generated from the contaminant source and mixed with the surrounding air, then joined the plume. It means that a large amount of supply reached breathing zone first and then mixed with contaminant (Figure 5.8b). The average concentration in breathing zone at PDV case 2 (0.75) was much better than completely mixing case.

In case 3, the supply air passed through person's legs once generated from diffuser because the buoyancy effect of person's legs were not strong enough to suck the air to the plume around person (Figure 5.5). Thus, the supply air reached contaminant

source first and mixed with contaminant, then blew back to join the plume (Figure 5.8c). The average concentration in breathing zone at PDV case 3 (1.03) was not much different from PDV case 1 (1.02).

In case 4 (DV), contaminant source mixed with room air after generated. Supply air fall down after generated from diffuser and traveled over floor, mixed with contaminant, then diffused to breathing zone (Figure 5.8d). The average concentration in breathing zone at case 4 (0.96) was also no much difference from completely mixing case.

In case A, we moved person and contaminant source closer to diffuser, but the average concentration in breathing zone did not decrease much. This is because contaminant was blown through person's legs by supply air and mixed with room air, then flew back to occupied zone as well as case 1 (Figure 5.8e). Thus, decreasing distance between person and diffuser will not help to decrease average concentration in breathing zone when contaminant source was located in front of person's feet.

In case B, we applied area source. Supply air mixed with contaminant which was on the floor at first and then passed through occupied zone. The average concentration in breathing zone (1.03) was not much different from completely mixing case.

In case C, direction of supply air was adjusted 45°up. As we discussed above, the ventilation bypass factor decreased accordingly (Table 5.2). However, the average concentration in breathing zone did not change because contaminant was still blown through person's legs by supply air after generated and then followed the same process with case 1, although supply air traveled longer before dropped to floor in case C. Thus,

adjusting direction of supply air will significantly decrease bypass factor, but will not help to decrease average concentration in breathing zone.

In case D, we added high panels around person. Area contaminant source was located on the floor. The average concentration in breathing zone (0.99) did not change much because supply air mixed with contaminant over the floor first and then traveled to join plume around person (Figure 5.8f). Thus, when area contaminant source is evenly located on the floor, adding high panels will not help much with decreasing average concentration in breathing zone.

In case E, point contaminant source was placed outside high panels and the local average concentration was the least (0.57) because the supply air reached breathing zone first and then mixed with the contaminant (Figure 5.8g). Thus, adding high panels will greatly help with decreasing average concentration in breathing zone when point contaminant source is located outside the panels.

In case F, floor supply ventilation was applied to compare with PDV. Area source was located on the floor which is the worst situation in floor supply ventilation. Supply air mixed with contaminant very well after generated from diffuser. The average concentration in breathing zone was 1 which is no worse than completely mixing case.

The local average contaminant concentration in breathing zone was high when the contaminant source was placed on the floor (case B, D and F) and in these cases, supply air mixed with contaminant first and then reached breathing zone.

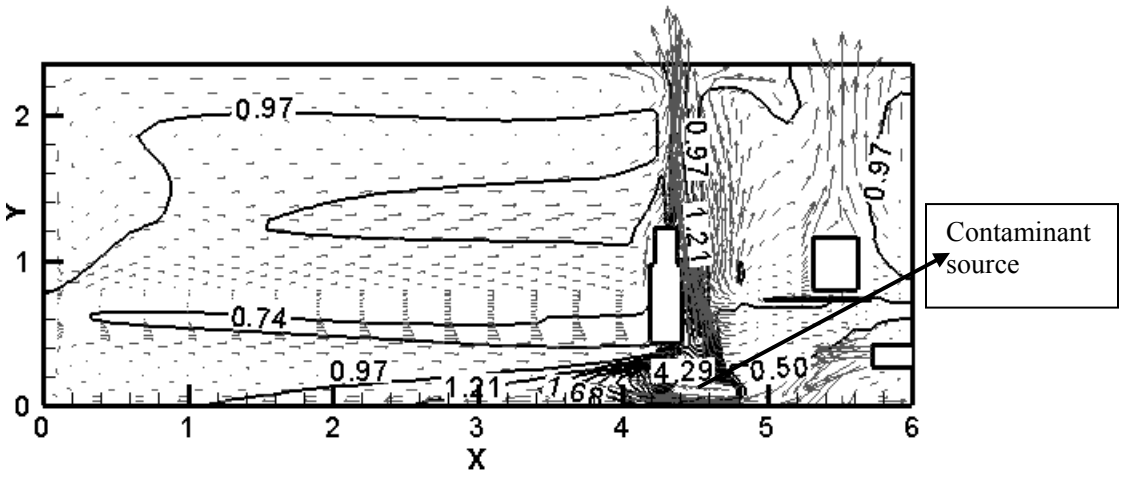

(a) Case 1 (PDV, point source)

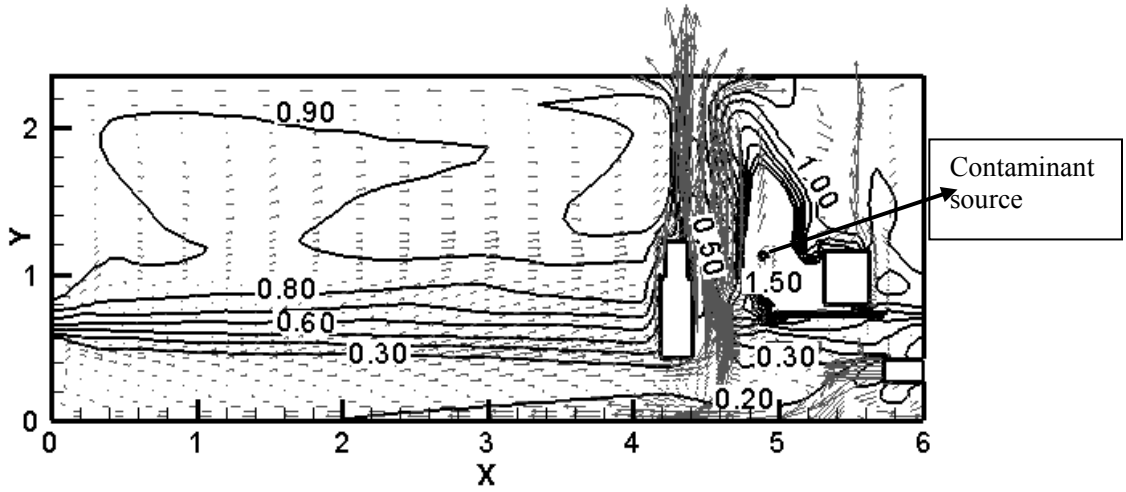

(b) Case 2 (PDV, point source)

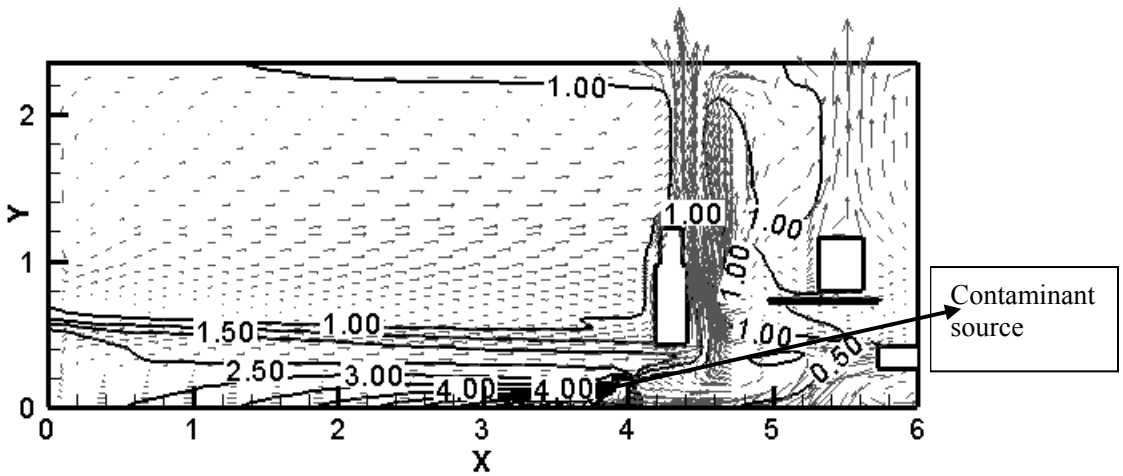

(c) Case 3 (PDV, point source)

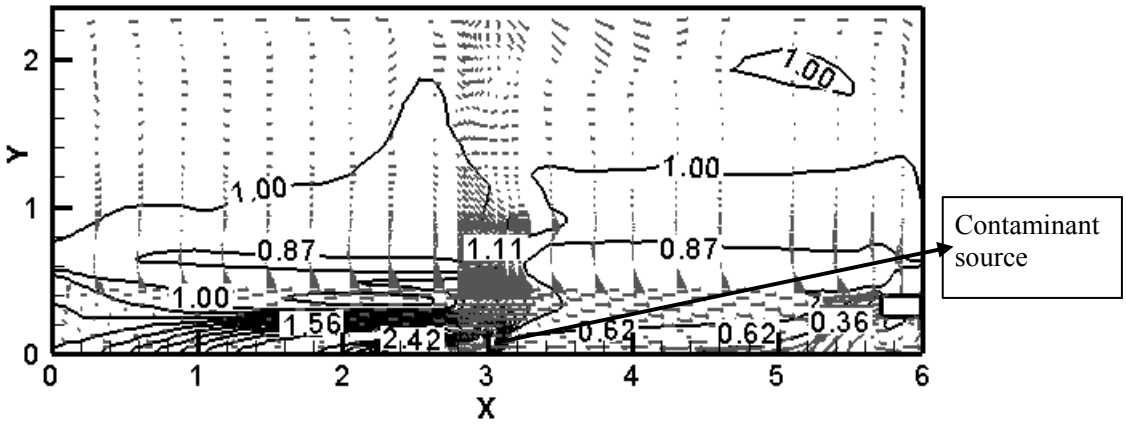

(d) Case 4 (DV, point source)

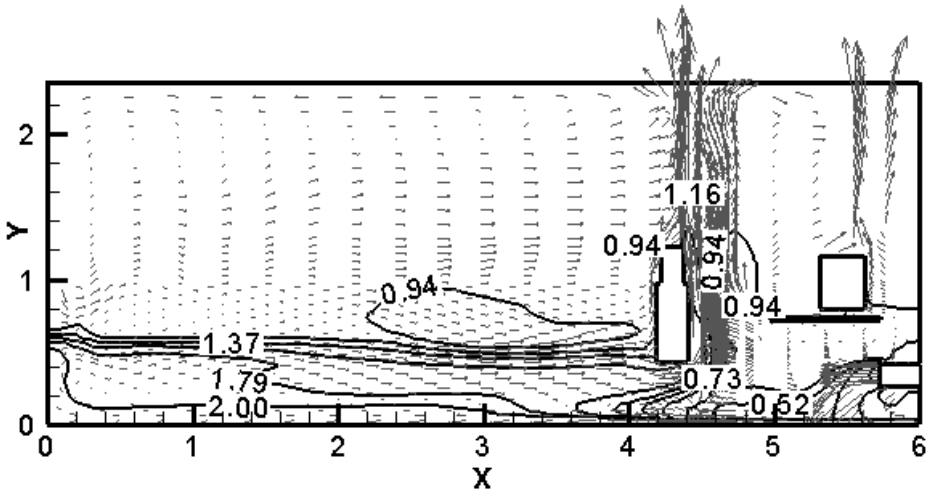

(e) Case A (area contaminant source on floor)

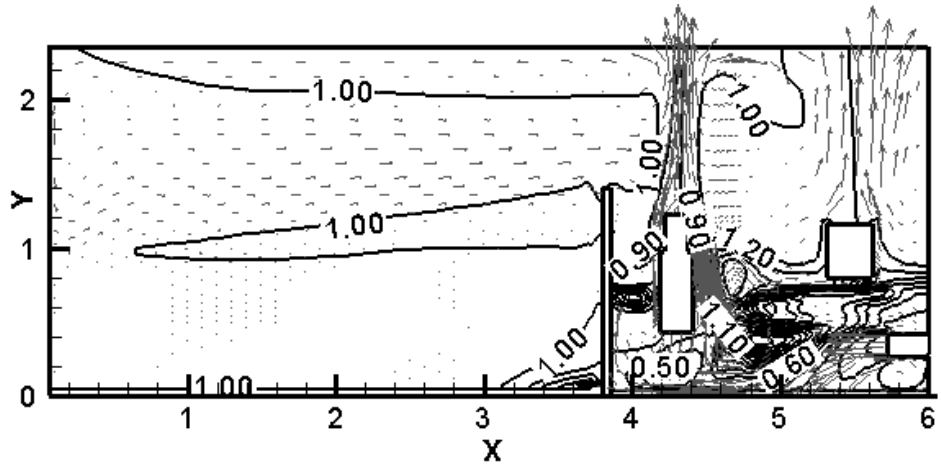

(f) Case D (area contaminant source on floor, high panels)

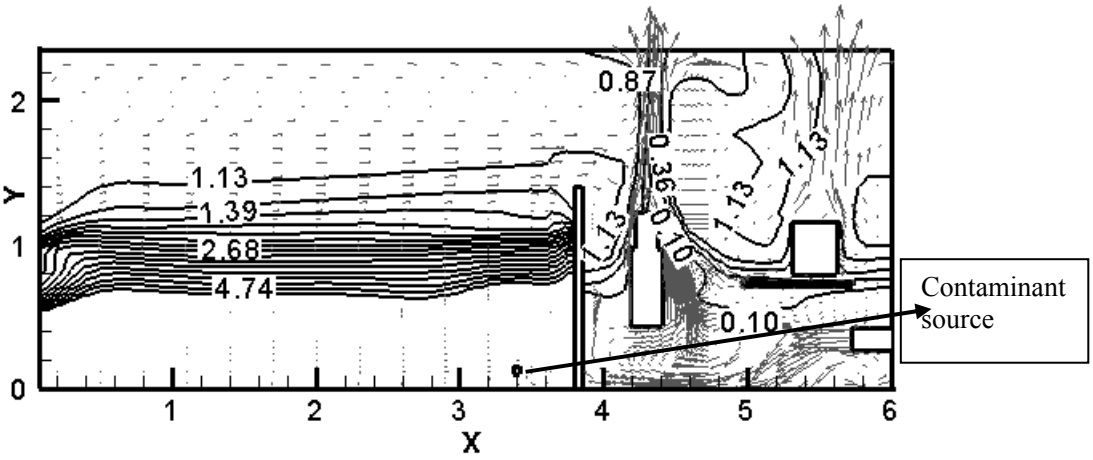

(g) Case E (point contaminant source, high panels)

Figure 5.8 Dimensionless iso-concentration contours and the velocity vector plot at room center z=1.95m in PDV cases.

5.4 Discussion of results

This chapter discusses ventilation cases by ventilation bypass factor and local average concentration. Air flow pattern and air quality in breathing zone are both evaluated. The results lead to following conclusions:

- Air flow pattern around person in PDV has not much difference from DV according to bypass factor analysis. This is because in PDV cases, supply air falls down to the floor after generated from diffuser due to the low flow rate of supply air. Since the buoyancy effect of person's legs is too small to suck up the air, supply air flows through person's legs, travels around floor and mixes with room air, then flows back to join the plume started from person's waist (Figure 5.5).

- Air quality in breathing zone is a crucial factor to evaluate the performance of a ventilation system, and it lies on many factors: air flow pattern, type of contaminant source, location of contaminant source and etc. Thus, it is very difficult but important for design engineer to predict local average concentration in breathing zone. In this chapter,

we provide a rule to generally predict local average concentration: When the supply air reaches breathing zone first and then mixes with contaminant, the local average concentration in breathing zone is relatively low, whereas, when supply air mixes with contaminant first and then reaches breathing zone, the local average concentration in breathing zone is relatively high.

- Placing high panels around person is the most efficient method to decrease the ventilation bypass factor and thus can greatly increase the fraction of supply air to join the plume around person. And it will greatly help with decreasing average concentration in breathing zone when point source was located outside the panel. However, it will not help much when area contaminant source is located evenly on the floor.

- Adjusting direction of supply air is effective on decreasing bypass factor and thus it can improve the fraction of supply air to join the plume around person, but it cannot help on decreasing average concentration in breathing zone..

- Decreasing the distance between person and inlet will not help on decreasing bypass factor or average concentration in breathing zone when contaminant source is located in front person's feet.

- To consider the worst situation in PDV, i.e., the contaminant source was place on floor when supply air mixes with contaminant first and then reaches breathing zone, the average contaminant concentration in PDV had no much difference from completely mixing case.

Chapter 6 Conclusions and Recommendations

This chapter presents main conclusions and results from this PDV research together with future recommendations.

6.1 Conclusions

The objective of this research is to evaluate PDV for indoor applications by using computational fluid dynamics (CFD) modeling and rigorous validation experiments. The associated work that has been done in this research includes:

- Experimental studies on the performance of PDV and DV systems with regard to airflow pattern, temperature distribution and contaminant concentration. (Chapter 3)
- Validation of CFD model. Comparison between simulation and experimental results is discussed. (Chapter 4)
- Validated CFD model is applied to simulate 6 more cases. Evaluation of these cases in addition to 4 experimental cases is achieved with two indicators: ventilation bypass factor and local average concentration. (Chapter 5)

The major conclusions from this study are summarized as follows.

- Basic equipped PDV acts no different from DV from airflow pattern's point of view. Due to the lack of heat generation around occupant's legs, local buoyancy effect is not strong enough to attract supply air, which is generated from diffuser nearby, to join in the plume around occupant. Thus, instead of rising up when reaches occupant's legs,

supply air flows through and travels over the floor until meets blockage; then rises up and travels back to join the plume beginning from the height of occupant's waist (Figure 5.5).

- Local average concentration in breathing zone can be predicted based on the relative locations of the supply air, contaminant source, and the person. When the supply air reaches breathing zone first and then mixes with contaminant, the local average concentration in breathing zone is relatively low, whereas, when supply air mixes with contaminant first and then reaches breathing zone, the local average concentration in breathing zone is relatively high.

- The performance of PDV system can be improved by employing auxiliary activities. Placing high panels around person is the most efficient method to decrease the ventilation bypass factor and thus can greatly increase the fraction of supply air to join the plume around person. And it will greatly help with decreasing average concentration in breathing zone when point source was located outside the panel. However, it will not help much when area contaminant source is located evenly on the floor.

- Adjusting direction of supply air is effective for decreasing the bypass factor and thus it can improve the fraction of supply air to join the plume around person, but it cannot help in decreasing the average concentration in breathing zone.

- Decreasing the distance between person and inlet will not help in decreasing bypass factor or average concentration in breathing zone when contaminant source is located in front of person's feet.

- Type and location of contaminant source can greatly affect local average contaminant concentration in breathing zone in PDV. However, even if under the worst

condition, average concentration in breathing zone in PDV has not much difference from a completely mixing ventilation system.

6.2 Recommendations for future research

To date, performance of ventilation systems is a significant problem owing to the development of modern technology and the desire of a healthy living and working environment. Since PDV has the advantage of saving energy and self-controlling microclimate at meantime, more researches on this topic needs to be carried out:

- Conduct more detailed experiments and modeling for complicated situations with multiple occupants and contaminant sources
- Evaluate combinations of PDV and other systems, for example, mixing ventilation or task conditioning system
- Evaluate the impacts of indoor activities, such as occupant's movement and respiration

References

Arpaci, V.S. and Larsen, P.S., 1984. Convection Heat Transfer, ISBN 0-13-172346-4.

Abbott, M.B. and Basco, D.R., 1989. Longman Scientific & Technical, ISBN 0-582-01365-8.

Awbi, H.B., 1991. Ventilation of Buildings, E & FN Spon, ISBN 0-419-15690-9.

Baker, A.J., Kelso, R.M., Gordon, E.B., Roy S. and Schaub E. G., 1997. Computational Fluid Dynamics: A two-edged sword. ASHRAE Journal, august, pp. 51-58.

Bauman, F., Arens, E.A., Fountain, M., Huizenga, C., et al., 1994. Localized thermal distribution for office buildings, final report - phase III, Center for Environmental Design Research, University of California, Berkeley, USA.

Bauman, F. and Arens, E.A., 1996. Task/Ambient conditioning systems: Engineering and application guidelines, CEDR-13-96, University of California, Berkeley, USA.

Benzinger, T.H., 1979. The Physiological basis for thermal comfort, Indoor Climate, ed. Fanger, P.O. and Valbjorn, O., pp.441-476, Danish Building Research Institute, Copenhagen, Denmark.

Brohus, H., and Nielson, P.V., 1996. Indoor Air 6: 157-167.

Brohus, H., 1997. Personal Exposure to Contaminant Sources in Ventilated Rooms, PhD Thesis, Aalborg, Department of Building Technology and Structural Engineering, Aalborg University, ISSN 0902–7953 R9741.

Bunn, R. et al., 1991. The future for cooling ceiling. Building Services Journal 13(11): 33–36

Bunn, R., 1996. Finding the right mix. Building Services Journal 18(8): 43–44

Cheesewright, R., King, K.J., and Ziai, S., 1986. Experimental data for the validation of computercodes for the prediction of two-dimensional buoyant cavity flows, Proc. ASME Meeting HTD, vol. 60 (heat transfer), pp.75-81.

Chen, Q., 1995. Numerical Heat Transfer, Part B, 28: 353-369.

Chen, Q., 1996. Building and Environment, 31(3): 233-244.

Chen, Q., 1997. ASHRAE Transactions 103(1): 178-187.

Cheong, K.W.D., Djunaedy, E., et al.. 2003. Building and Environment 38: 135-145.

Dickson, D., 1994. A testing time for chilled ceiling. Building Services Journal 16(6): 31–32

Fanger, P.O., 1999. Indoor Environment in the 21st century - search for the optimal. VVS Danvak, 5. April: 10-14

Fluent, Inc. 1996. User's Guide for Fluent/UNS & Rampant, release 4.0, Lebanon, USA.

Fluent, Inc. 1996. Tgrid User's Guide release 2.4, Lebanon, USA.

Gao, N. and Niu J., 2004. CFD study on micro-environment around human body and personalized ventilation. Building and Environment 39(2004): 795-805

Hagstrom, K., Zhivov, A.M., et al., 1999. ASHRAE Transactions 105(2): 750-758.

Hagstrom, K., Zhivov A.M., et al., 2002. Building and Environment 37: 55-66.

He, G. and Yang, X., ASHRAE Transaction 2005, (1): 646-652

He, G., Yang, X., and Srebric, J., 2005. Indoor Air 15: 367-380

Ji, Y. et al., 2007. Building and Environment 42(3): 1158-1172

Krantz, 1984. "Air distribution systems," Report No. 3554E, Krantz Products, Colchester, UK.

Lau, J. and Chen, Q., 2007. "Floor-supply displacement ventilation for workshops," Building and Environment, 42(4): 1718-1730

Launder, B.E. and Spalding, D.B., 1974. Computer Methods in Applied Mechanics and Energy, 3: 268-289.

Liu, Z., Zhao, B., Yang, X., 2006. A Method for Calculating Ventilation Bypass Factor. Indoor Air. Submitted on May 31, 2006

Loomans, M., 1998. The Measurement and Simulation of Indoor Air Flow. PhD. Thesis. The Netherlands: University of Eindhoven, ISBN 90 6814 085 X

Nielsen, P.V., Restivo, A. and Whitelaw, J.H., 1978. The velocity characteristics of ventilated rooms, Journal of Fluid Engineering, vol.100, pp.291-298.

Patankar, S.V., 1980. Numerical Heat Transfer and Fluid Flow. Hemisphere Publishing Corporation, USA.

Salisbury, S.A., 1989. “Evaluating building ventilation for indoor air quality investigations,” The Practitioner’s Approach to Indoor Air Quality Investigations – Proceedings of the Indoor Air Quality International Symposium, 87-98. American Industrial Hygiene Association, Fairfax, VA

Sandberg, M., and Etheridge, D., 1996. Building Ventilation: Theory & Measurement. New York: John Wiley & Sons.

Seitz, T.A., 1989. Indoor Air QualityInternational Symposium, 163-171. American Industrial Hygiene Association, Fairfax, VA.

Srebric, J. and Chen Q., 2002. HVAC&R Research 8(3): 277-294.

Tennekes, H. and Lumley, J.L., 1972. A first Course in Turbulence, MIT Press, Cambridge, Massachusetts, USA.

Tuddenham D., 1985. ASHRAE Transactions **91** (1): 387–403.

Turiel, I., 1985. Indoor Air Quality and Human Health , Stanford University Press, Stanford, California, USA.

Yakhot, V., Orzag S.A., et al., 1992. Phys. Fluids A, 4(7): 1510-1520.

Yang, X. and Srebric, J., 2001. CLIMA 2000 Conference, Napoli, Italy, September 15-18, 2001.

Yang X., Srebric J., et al., 2004. Building and Environment 39: 1289-1299

Yuan X., Chen Q. and Glicksman L.R., 1998. ASHRAE Transactions 104 (1A): 78–90.

Yuan, X., Chen Q., et al., 1999. ASHRAE Transactions 105(1): 340-352

Zhang, L. and Chow, T.T., 2005. Building and Environment 40(8): 1051-1067

Appendix A Room configuration in experimental cases

A.1 PDV cases

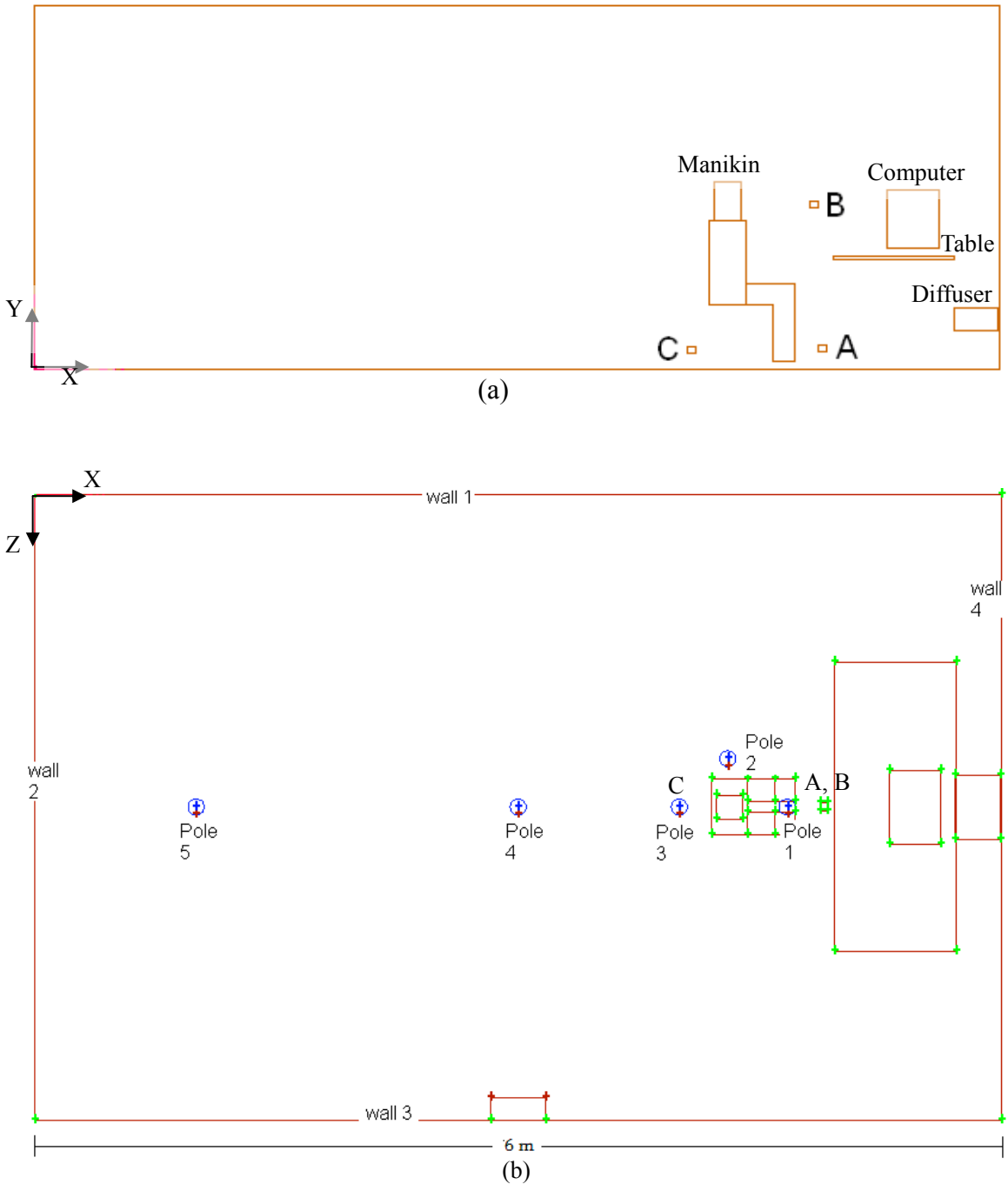

Figure A.1 Layout of PDV test cases. A, B, C represent different contaminant source locations respectively. Pole 1~ Pole 5 represent different measurement locations.

Table A.1 Room configuration in PDV cases

Name	Location (m)			Size (m)			Heat (W)
	x	y	z	Δx	Δy	Δz	
Room	0	0	0	6	2.35	3.9	0
Diffuser	5.72	0.27	1.75	0.28	0.15	0.4	0
Computer	5.31	0.79	1.72	0.31	0.37	0.46	40
Table	4,97	0.72	1.04	0.76	0.025	1.82	0
Person	4.19	0.055	1.78	0.52	1.18	0.35	76
Source A	4.87	0.11	1.93	0.05	0.05	0.05	0
Source B	4.87	1.11	1.93	0.05	0.05	0.05	0
Source C	4	0.11	1.93	0.05	0.05	0.05	0

A.2 DV case

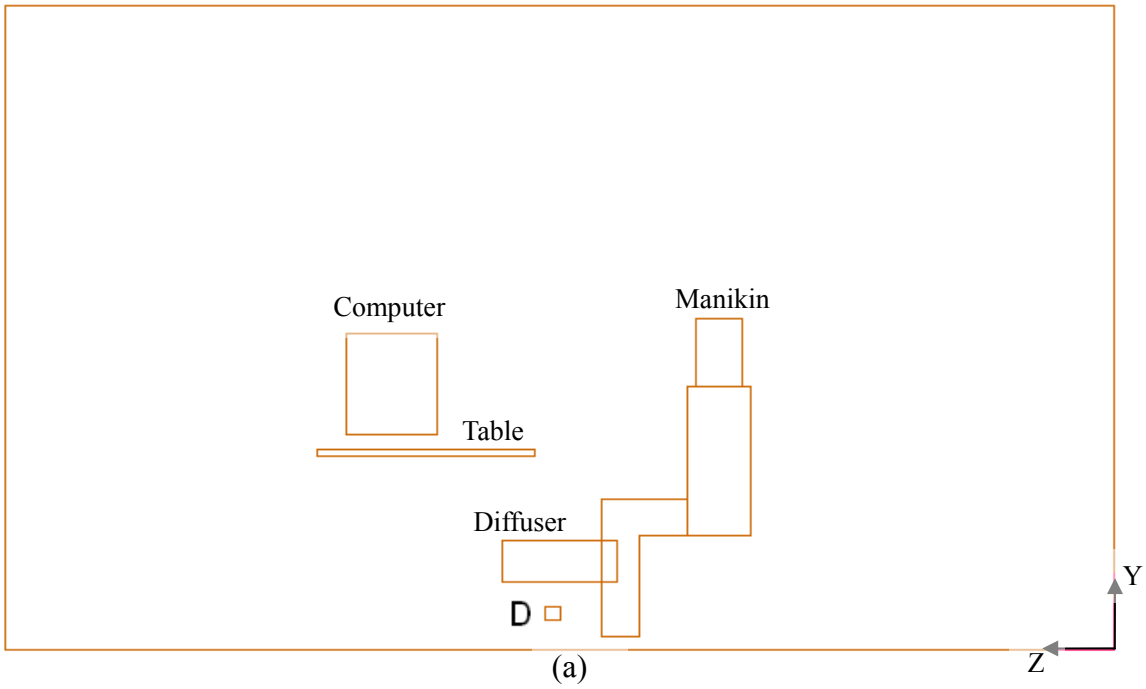

(a)

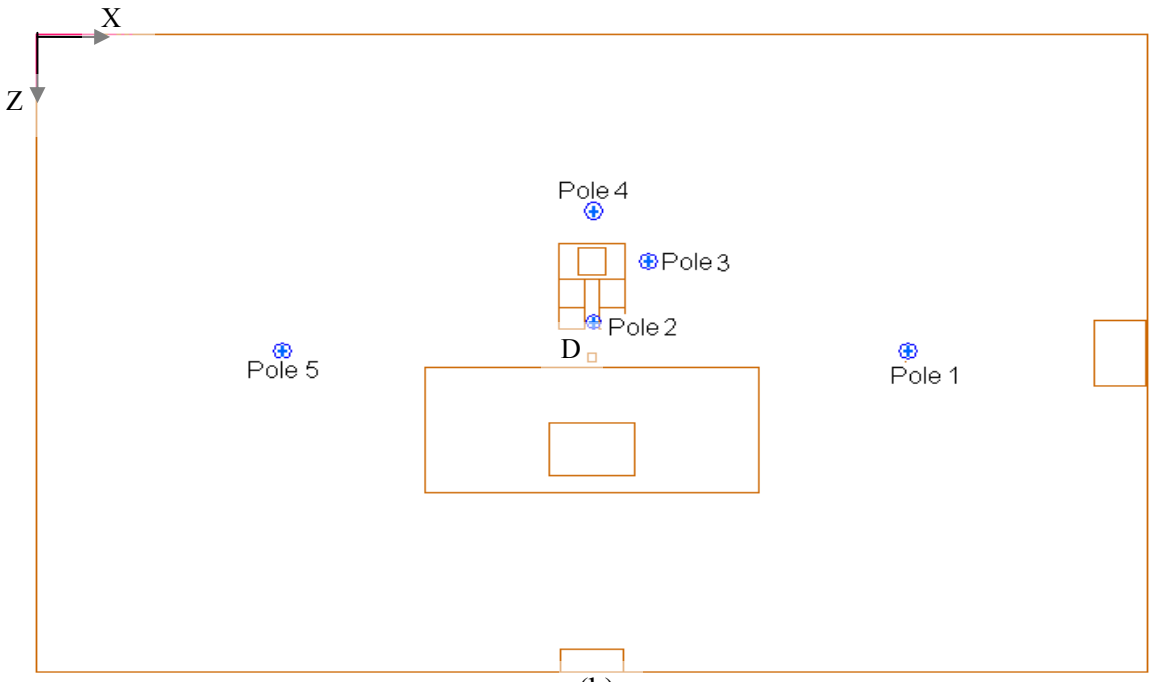

(b)

Figure A.2 Layout of DV test case. D represents contaminant source location. Pole 1~ Pole 5 represent different measurement locations.

Table A.2 Room configuration in DV case

Name	Location (m)			Size (m)			Heat (W)
	x	y	z	Δx	Δy	Δz	
Room	0	0	0	6	2.35	3.9	0
Diffuser	5.72	0.27	1.75	0.28	0.15	0.4	0
Computer	2.77	0.79	2.38	0.46	0.37	0.31	40
Table	2.1	0.72	2.04	1.82	0.025	0.76	0
Person	3.18	0.055	1.28	0.35	1.19	0.52	76
Source D	3.03	0.11	1.95	0.05	0.05	0.05	0